7th Nano and Giga Challenges in Electronics, Photonics and Renewable Energy
Tomsk State University (Russia), September 8-22, 2017

Theoretical Study on Energy Conversion Processes of Perovskite Solar Cells

Koichi Yamashita

Department of Chemical System Engineering,
The University of Tokyo, Japan

Computational Materials Science For Energy Conversion

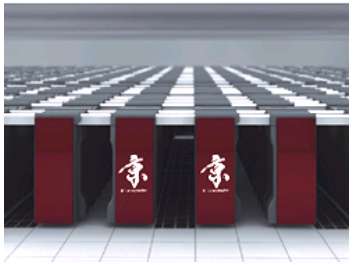

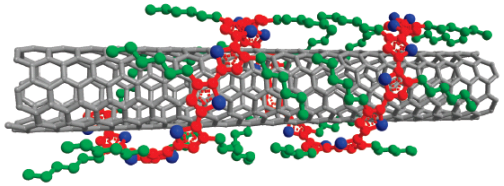

Organic Photovoltaic Cells

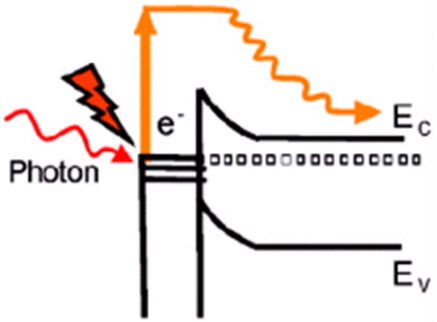

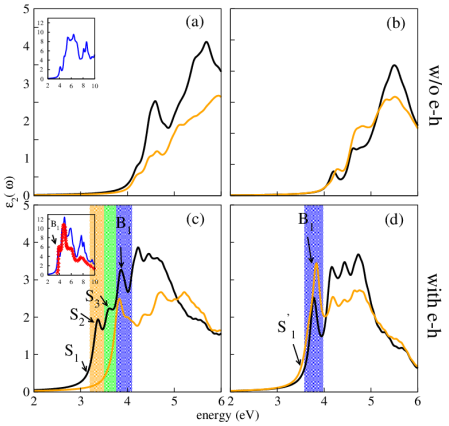

Photocatalysis

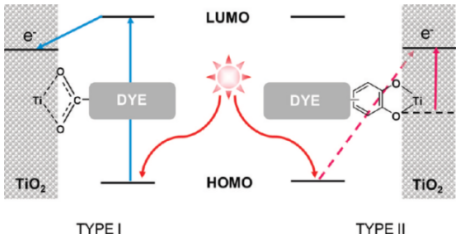

Dye-Sensitized Solar Cells

Interfacial Carrier Transport

Rechargeable Battery

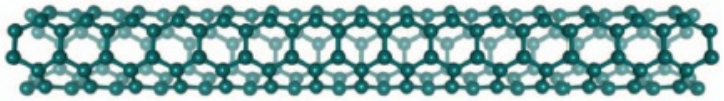

Thermal Transport

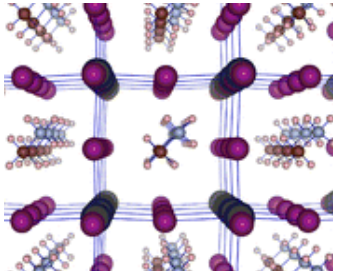

Perovskite Photovoltaics

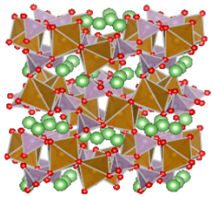

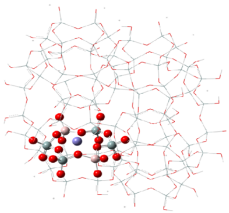

Automobile Catalysis

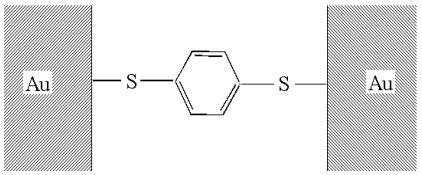

Molecular Electronics

Perovskite Photovoltaics

Jin Hyuck Heo[1†], Sang Hyuk Im[1,2†], Jun Hong Noh[1†], Tarak N. Mandal[1], Choong-Sun Lim[1], Jeong Ah Chang[1], Yong Hui Lee[1], Hi-jung Kim[1], Arpita Sarkar[1], Md. K. Nazeeruddin[3], Michael Grätzel[3*] and Sang Il Seok[1,4*]

Nature Photonics 5 May 2013

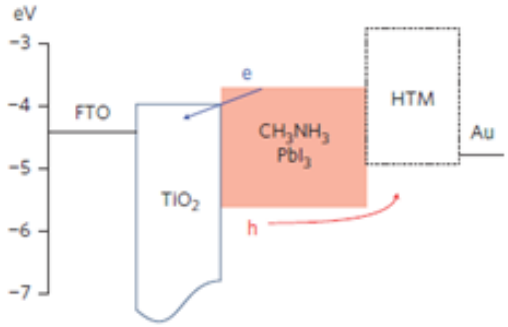

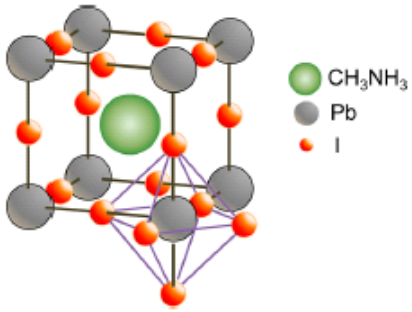

Michael M. Lee,[1] Joël Teuscher,[1] Tsutomu Miyasaka,[2] Takurou N. Murakami,[2,3] Henry J. Snaith[1*]

SCIENCE 5 November 2012

$MAPbI_3$ perovskite compounds as a light harvester (Miyasaka *et al.*, JACS 2009)

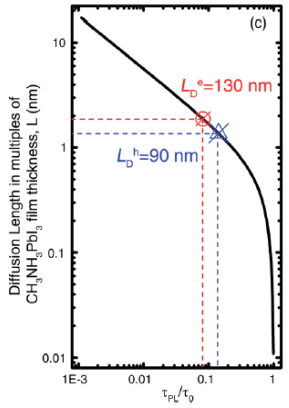

Key Properties:

- Ambipolar Charge Transfer
- Long Charge Carrier Lifetime and Diffusion Length

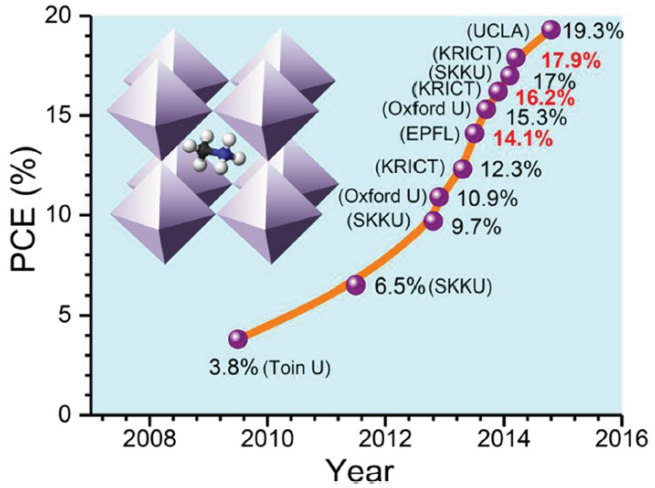

~22%

Xing *et al.*, Science (2013)

Photocarrier Effective Mass

Giorgi, Fujisawa, Segawa, Yamashita, JPCL(2013) ***4****, 4213*

DFT/PBE,PAW

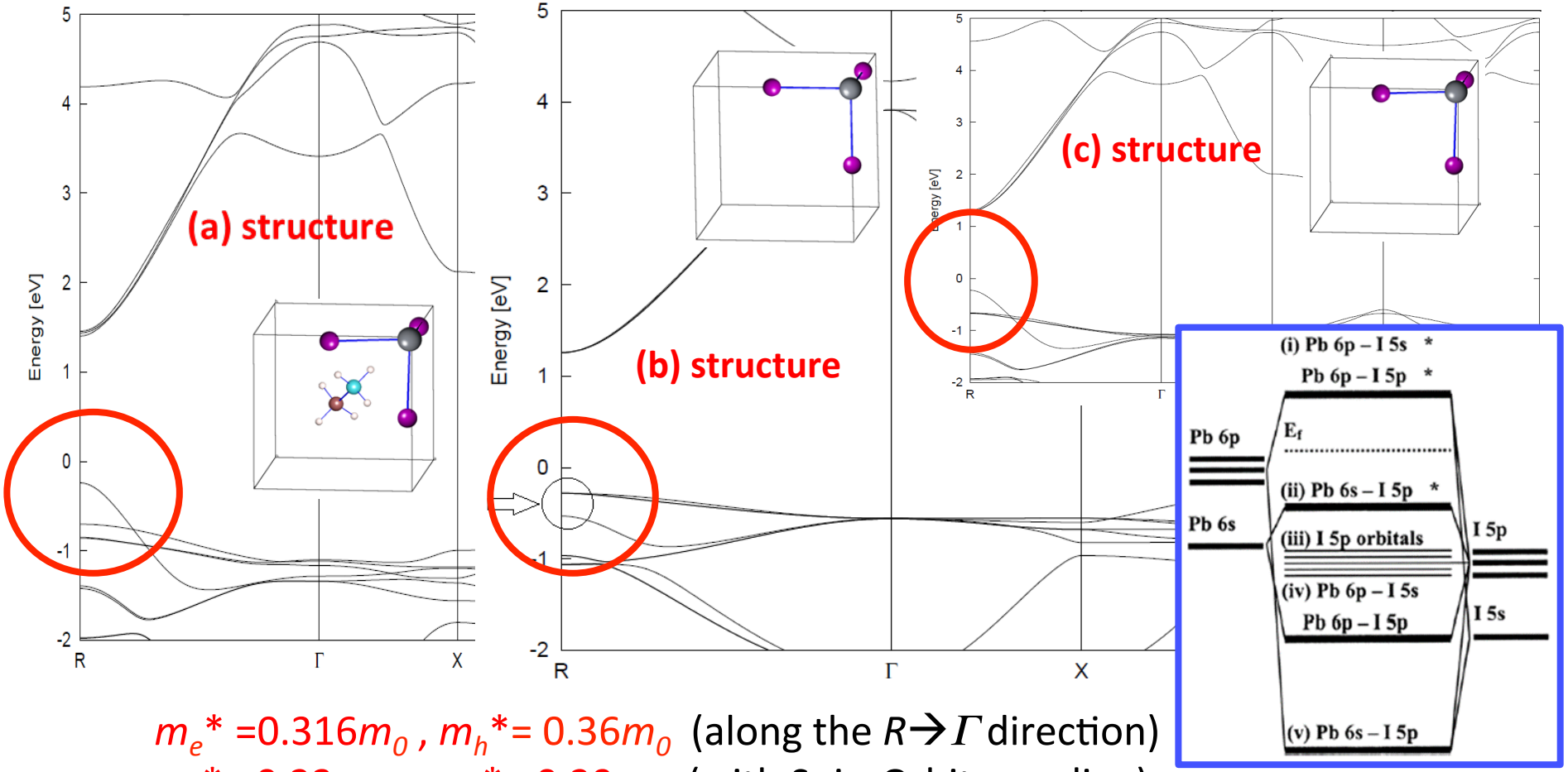

$m_e^* = 0.316 m_0$, $m_h^* = 0.36 m_0$ (along the $R \rightarrow \Gamma$ direction)

$m_e^* = 0.23\ m_0$, $m_h^* = 0.29 m_0$ (with Spin-Orbit coupling)

This result clearly reveals the ambipolar nature of the material

MA induces the ambipolar (hole-transport) behavior

Giorgi, Fujisawa, Segawa, Yamashita, JPCC(2014) ***118****, 12176*

Long-Range Balanced Electron- and Hole-Transport Lengths in Organic-Inorganic $CH_3NH_3PbI_3$

18 OCTOBER 2013 VOL 342 SCIENCE

Guichuan Xing,[1]* Nripan Mathews,[2,3,4]*† Shuangyong Sun,[2] Swee Sien Lim,[1] Yeng Ming Lam,[2,5] Michael Grätzel,[3,6] Subodh Mhaisalkar,[2,3] Tze Chien Sum[1]†

Exceed theoretical Shockley-Queisser limit ?

Transient Absorption Measurement

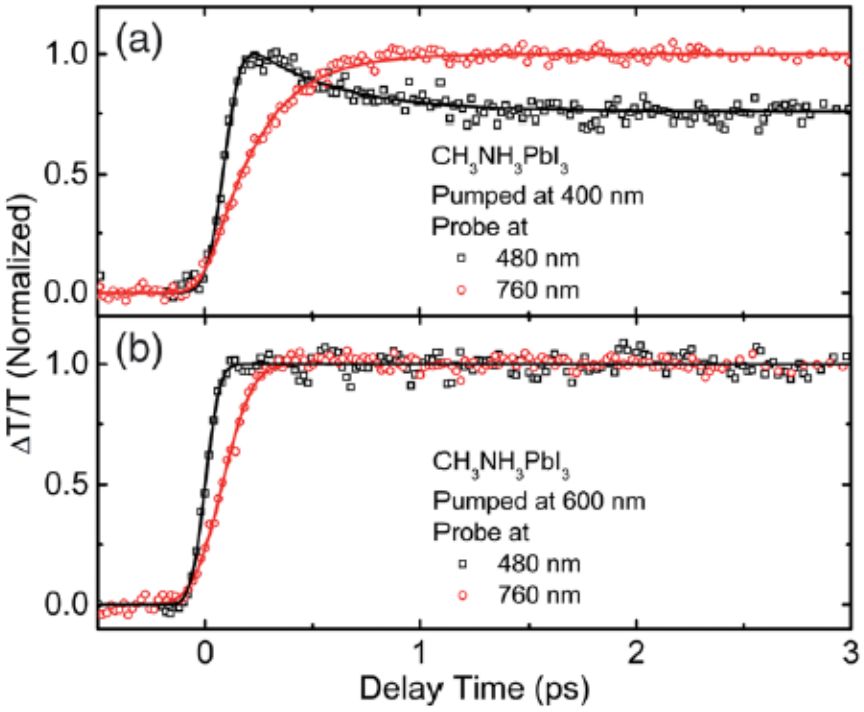

"This 0.4-ps hot-hole cooling is much slower than that in most organic semiconductors (~100 fs)"

Hot "Carrier (Hole)"

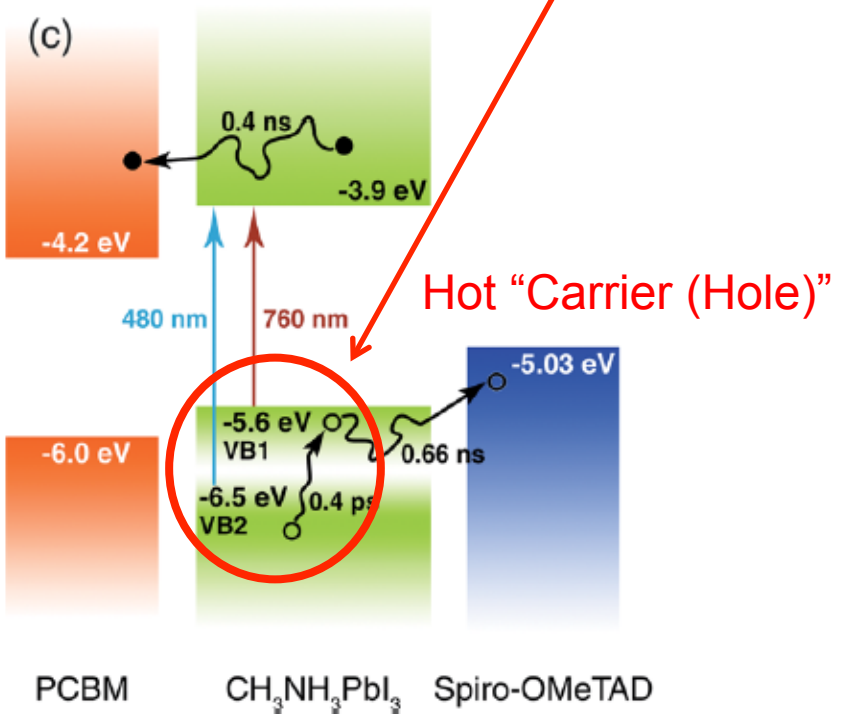

Carrier Relaxation Lifetime

$$\tau_{n\mathbf{k}}^{-1} = 2\mathrm{Im}\Sigma_{n\mathbf{k}}^{\mathrm{Fan}}(\varepsilon_{n\mathbf{k}}, T = 0\mathrm{K})$$

$$\approx \begin{cases} \dfrac{2}{N_{\mathbf{q}}} \sum_{\mathbf{q}\lambda} \sum_{n' \in \mathrm{CB}} \left| g_{nn'\mathbf{k}}^{\mathbf{q}\lambda} \right|^2 \delta(\varepsilon_{n\mathbf{k}} - \varepsilon_{n'\mathbf{k}-\mathbf{q}} - \omega_{\mathbf{q}\lambda}) & \text{Phonon emission } n \in \mathrm{CB} \\ \dfrac{2}{N_{\mathbf{q}}} \sum_{\mathbf{q}\lambda} \sum_{n' \in \mathrm{VB}} \left| g_{nn'\mathbf{k}}^{\mathbf{q}\lambda} \right|^2 \delta(\varepsilon_{n\mathbf{k}} - \varepsilon_{n'\mathbf{k}-\mathbf{q}} + \omega_{\mathbf{q}\lambda}) & \text{Phonon absorption } n \in \mathrm{VB} \end{cases}$$

$N_{\mathbf{q}}$: Number of q-points

$g_{nn'\mathbf{k}}^{\mathbf{q}\lambda}$: e-ph coupling

$\omega_{\mathbf{q}\lambda}$: Phonon frequency

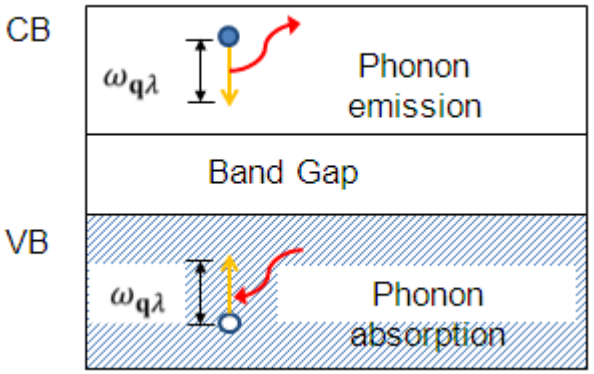

Generalized Eliashberg function:

$$\mathrm{g}F_{n\boldsymbol{k}}^2(\omega)\big|_{\mathrm{Fan}} = \frac{1}{N_q} \sum_{n'\mathbf{q}\lambda} \frac{\left| g_{nn'\mathbf{k}}^{\mathbf{q}\lambda} \right|^2}{\varepsilon_{n\mathbf{k}}^{KS} - \varepsilon_{n'\mathbf{k}-\mathbf{q}}^{KS}} \left[2N_{\mathbf{q}\lambda}(T) + 1 \right] \delta(\omega - \omega_{\mathbf{q}\lambda})$$

H. Kawai, G.Giorgi, A. Marini, K. Yamashita, *Nano Lett.*, ***15***, *3103-3108* (2015)

Lifetime and DOS

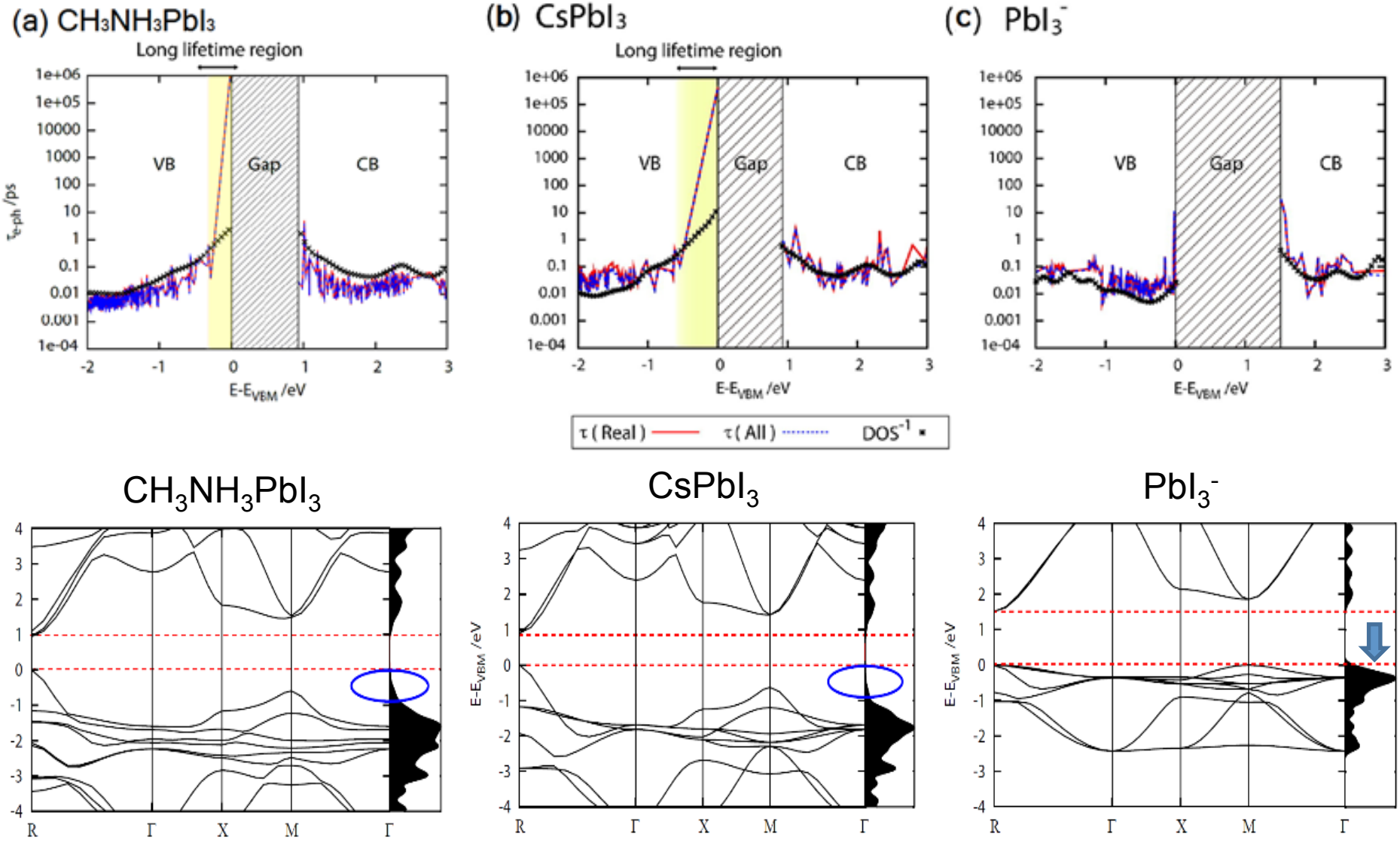

H. Kawai, G.Giorgi, A. Marini, K. Yamashita, *Nano Lett., 15, 3103-3108* (2015)

Electron-Phonon Coupling

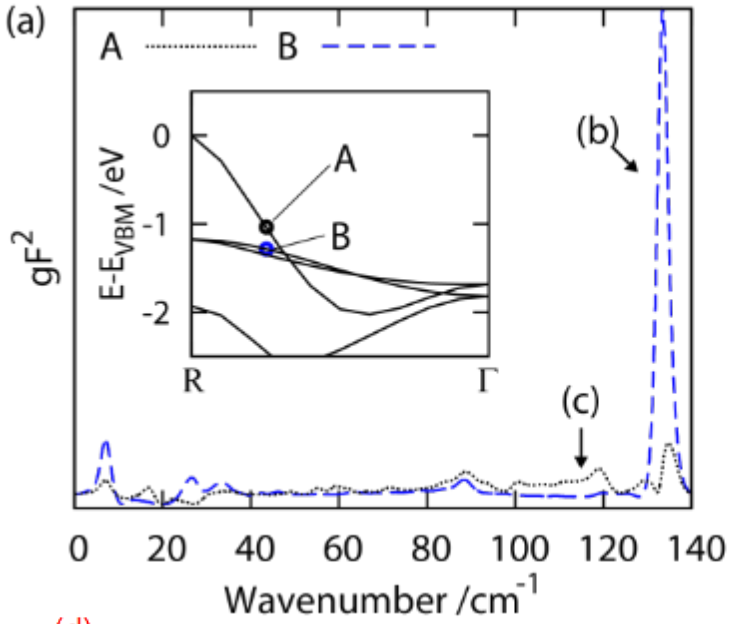

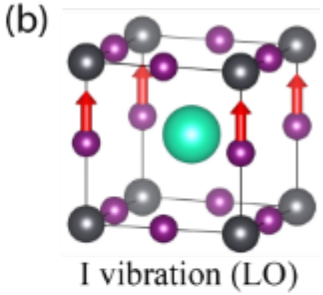

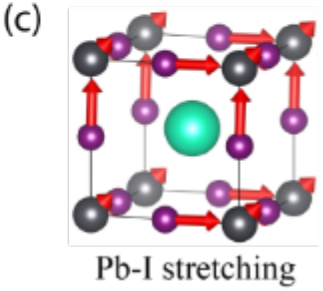

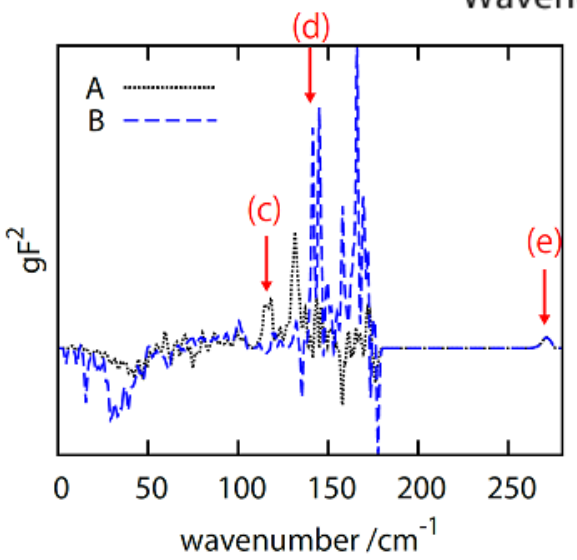

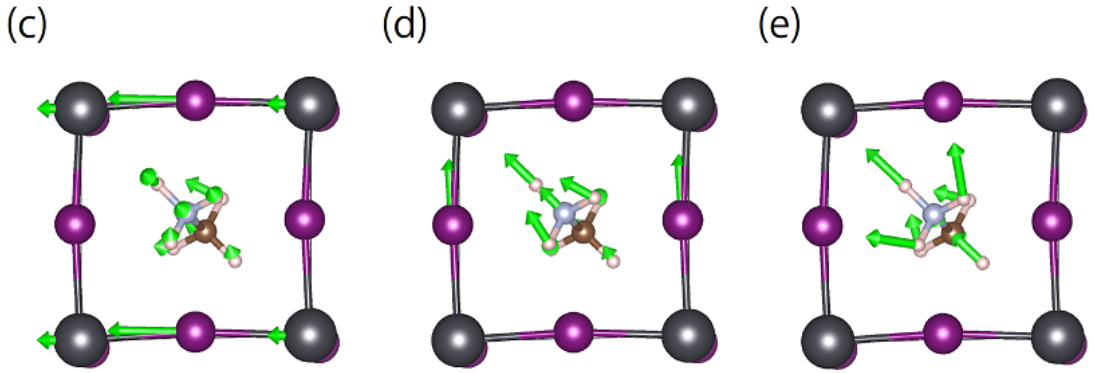

H. Kawai, G.Giorgi, A. Marini, K. Yamashita, *Nano Lett., 15, 3103-3108* (2015)

Hot-Hole Cooling

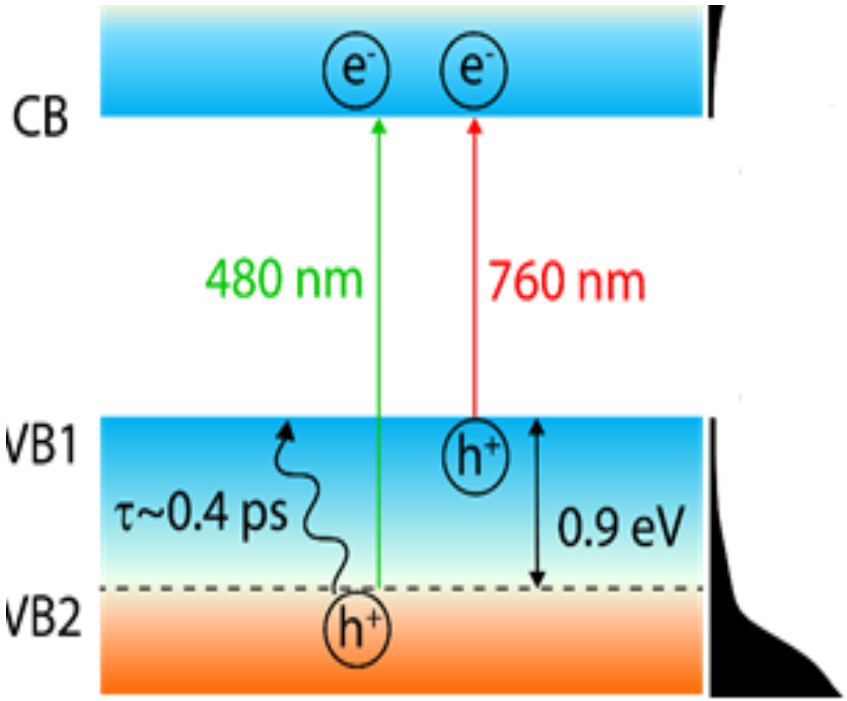

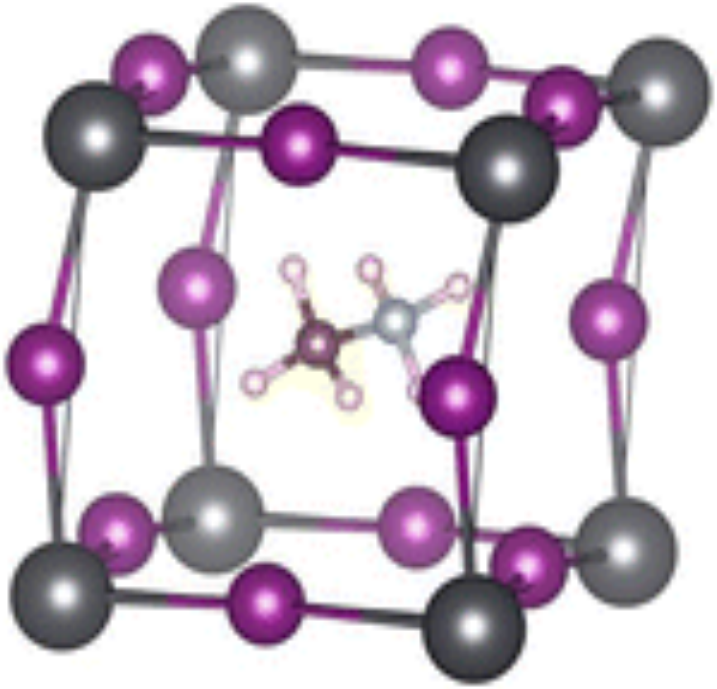

■ A reduction of the relaxation paths in the small valence DOS as being the origin of the slow hot-hole cooling.

H. Kawai, G.Giorgi, A. Marini, K. Yamashita, *Nano Lett., 15, 3103-3108* (2015)

Photophysical Processes and Loss Mechanism

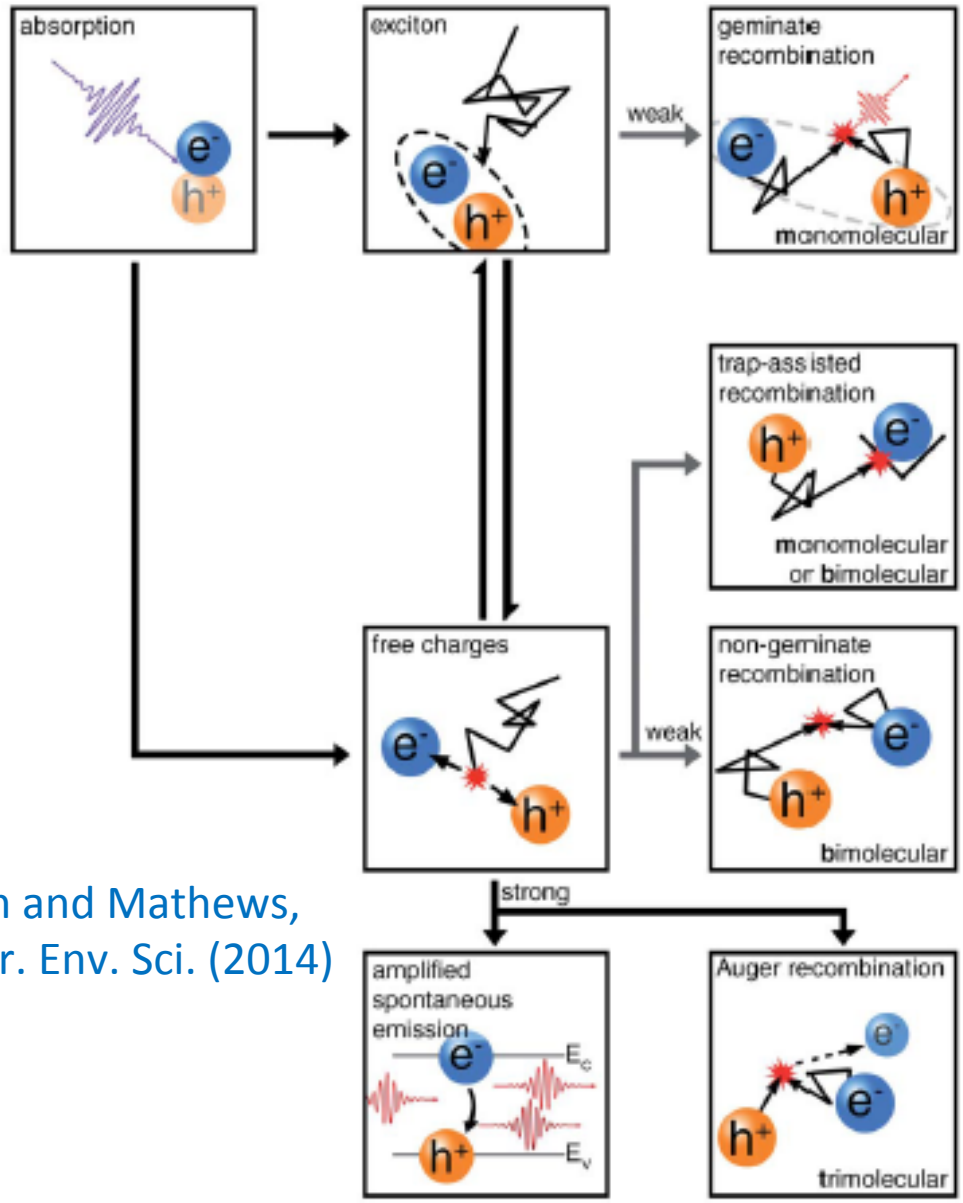

Sum and Mathews, Ener. Env. Sci. (2014)

Free-carrier model

Yamada et al. JACS (2014)

PL and TA measurements

E_b~25-37meV

Miyata et al. Nat. Phys. (2015)

Very high magnetic field

E_b~16meV (low temp)

reduced effective mass 0.104m_e

Phase transition

at 160 K

orthorhombic → tetragonal

at 330 K (k_BT~25 meV)

tetragonal →cubic

Long charge carrier lifetime and diffusion length

Combination of

- high charge carrier mobilities
- **low charge carrier recombination rates**

$MAPbI_3$ is characterized by

- Strong absorption constant
- High photoluminescence quantum yield

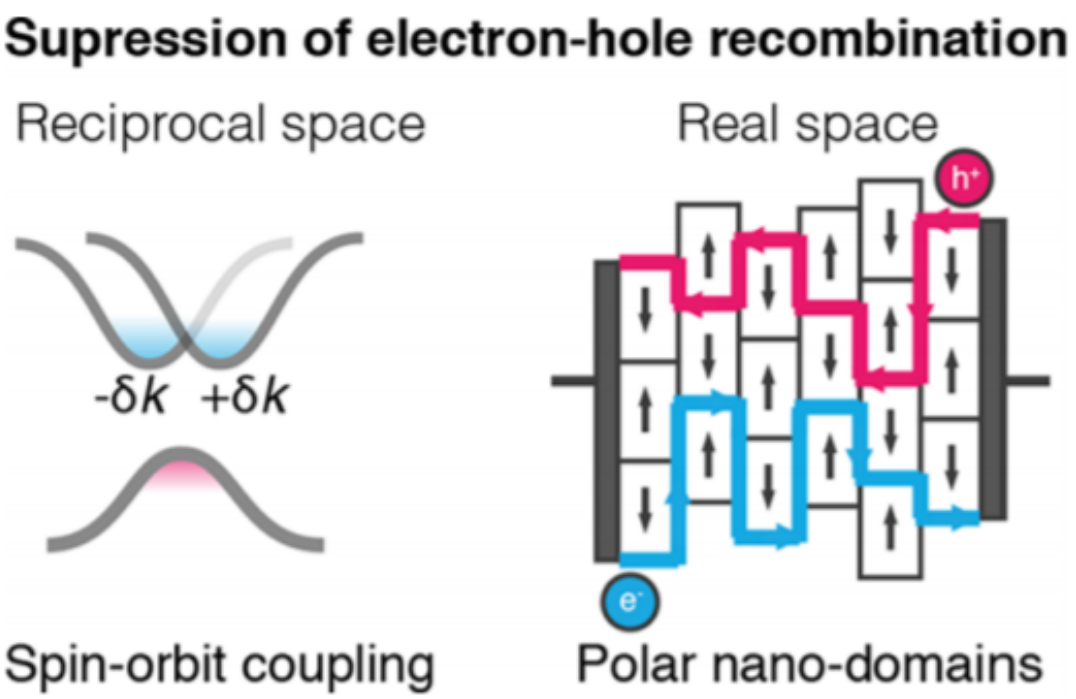

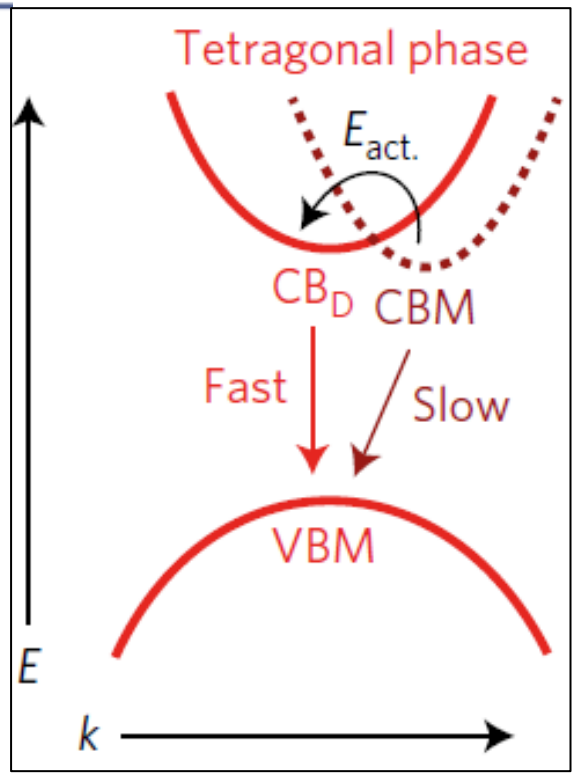

Rashba effect

Ferroelectric effect

Direct-indirect bandgap

Frost and Walsh, *Acc. Chem. Res.*, **49**, 528 (2016)

Hutter et al,
Nat. Mater., **16**, 115 (2017)

$MAPbI_3$ Clusters

Top view

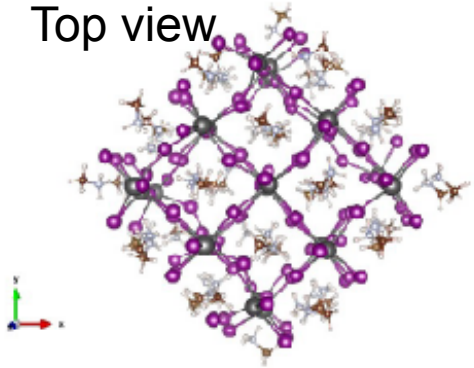

Lateral view

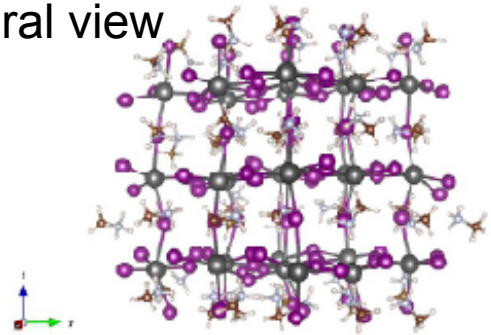

1s cluster

$MA_{54}Pb_{27}I_{108}$ (567 atoms)

Cubic-like, MAI-terminated

organic/inorganic cation ratio = 2.00

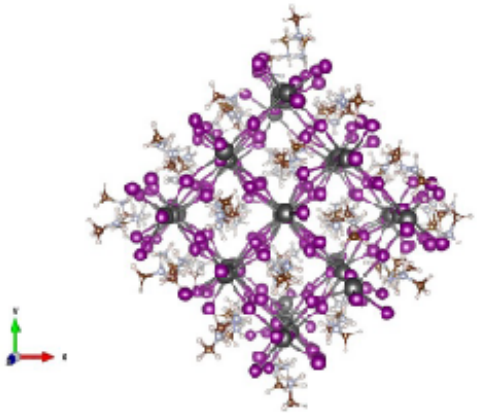

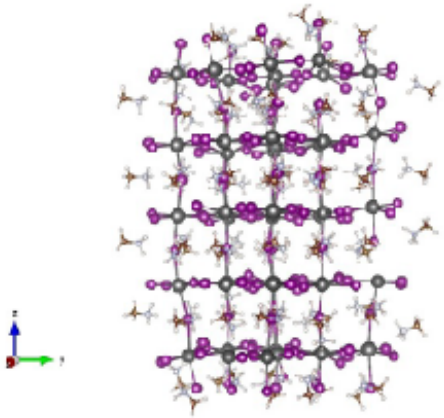

2i cluster

$MA_{84}Pb_{45}I_{174}$ (891 atoms)

Tetragonal-like, MAI-terminated

organic/inorganic cation ratio = 1.87

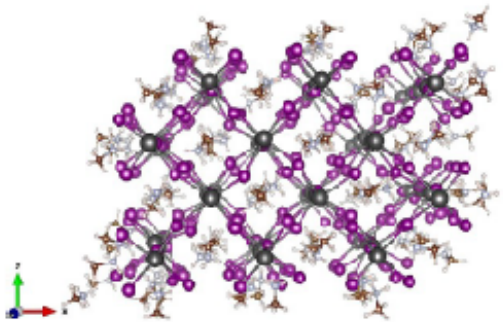

Gray, Pb;
purple, I;
brown, C;
light blue, N;
white, H

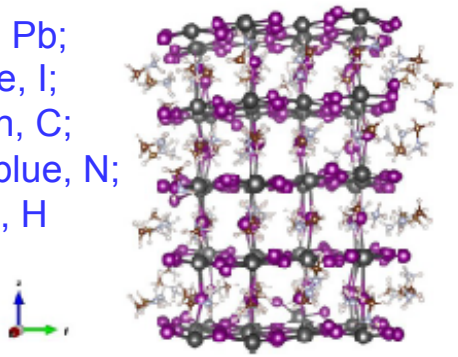

3l cluster

$MA_{93}Pb_{60}I_{213}$ (1017 atoms)

[001] facet: PbI_2-termonated

[100], [010]; MAI-terminated

organic/inorganic cation ratio = 1.55

Trajectory of *1s* cluster

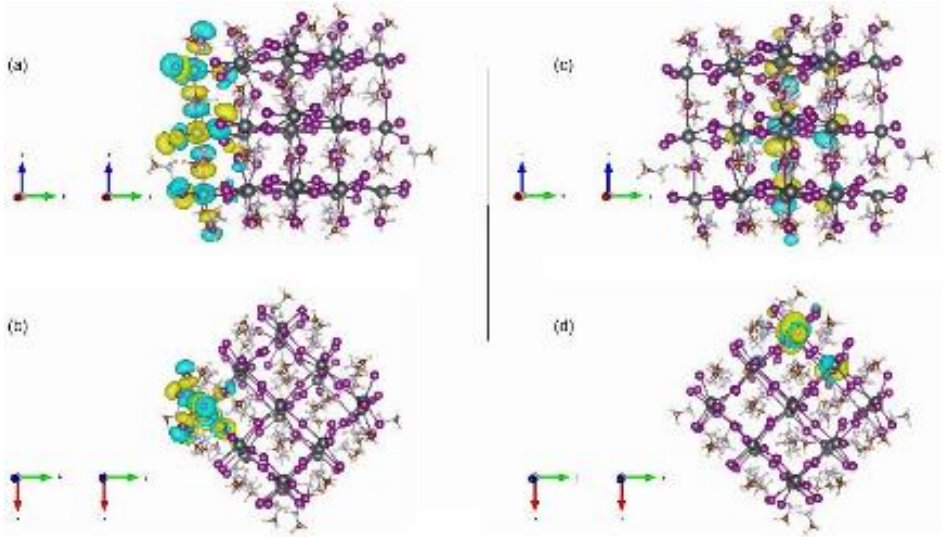

(a) Side and (b) top view of the VBM (**2.05**ps).(c) and (d) same for the CBM.

Both VBM and the CBM are spread along the surface edge.

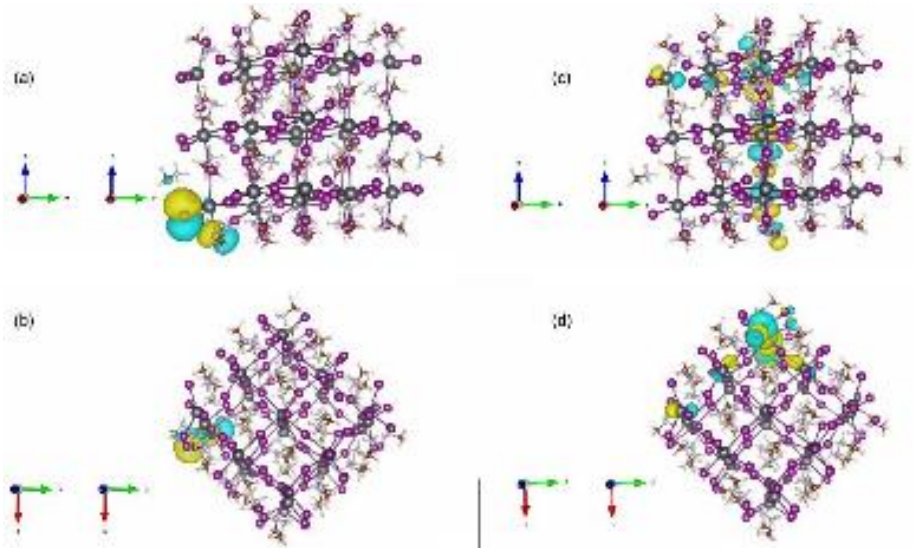

(a) Side and (b) top view of the VBM (**2.85**ps). (c) and (d) same for the CBM.

VBM is mainly localized into a single PbI_6 octahedron at the surface.
CBM is more spread along one of the ⋯Pb−I−Pb⋯ edges in the z direction.

We can expect that an efficient electron (CBM)−hole (VBM) separation takes place, proving a reduced tendency of recombination once the cluster is excited.

G. Giorgi, K. Yamashita, *J. Phys. Chem. Lett.*, **7**, 888-899 (2016)

Trajectory of *2i* cluster

G. Giorgi, K. Yamashita, *J. Phys. Chem. Lett.*, **7**, 888-899 (2016)

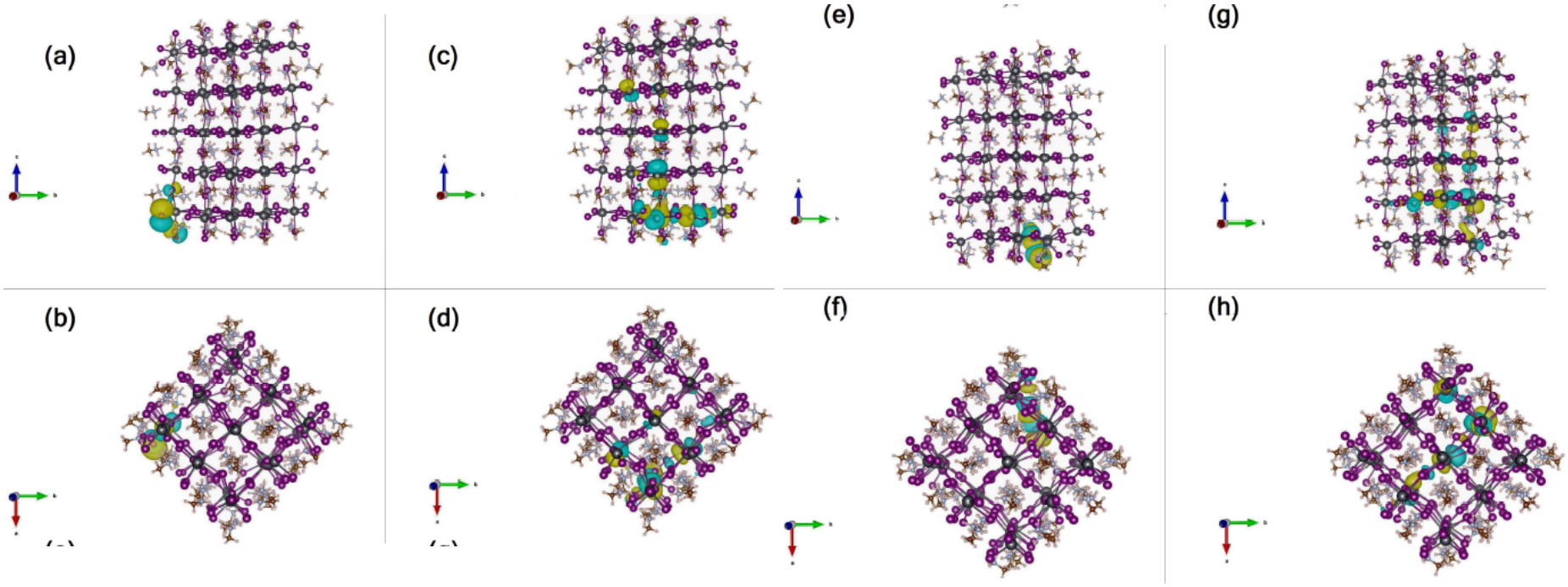

(a) Lateral and (b) top view of the VBM after 2.65 ps (2.10 eV)
(c) and (d) for the CBM.
(e) Lateral and (f) top view for the VBM after 0.90 ps (1.46 eV)
(g) and (h) for the CBM

Trajectory of *3I* cluster

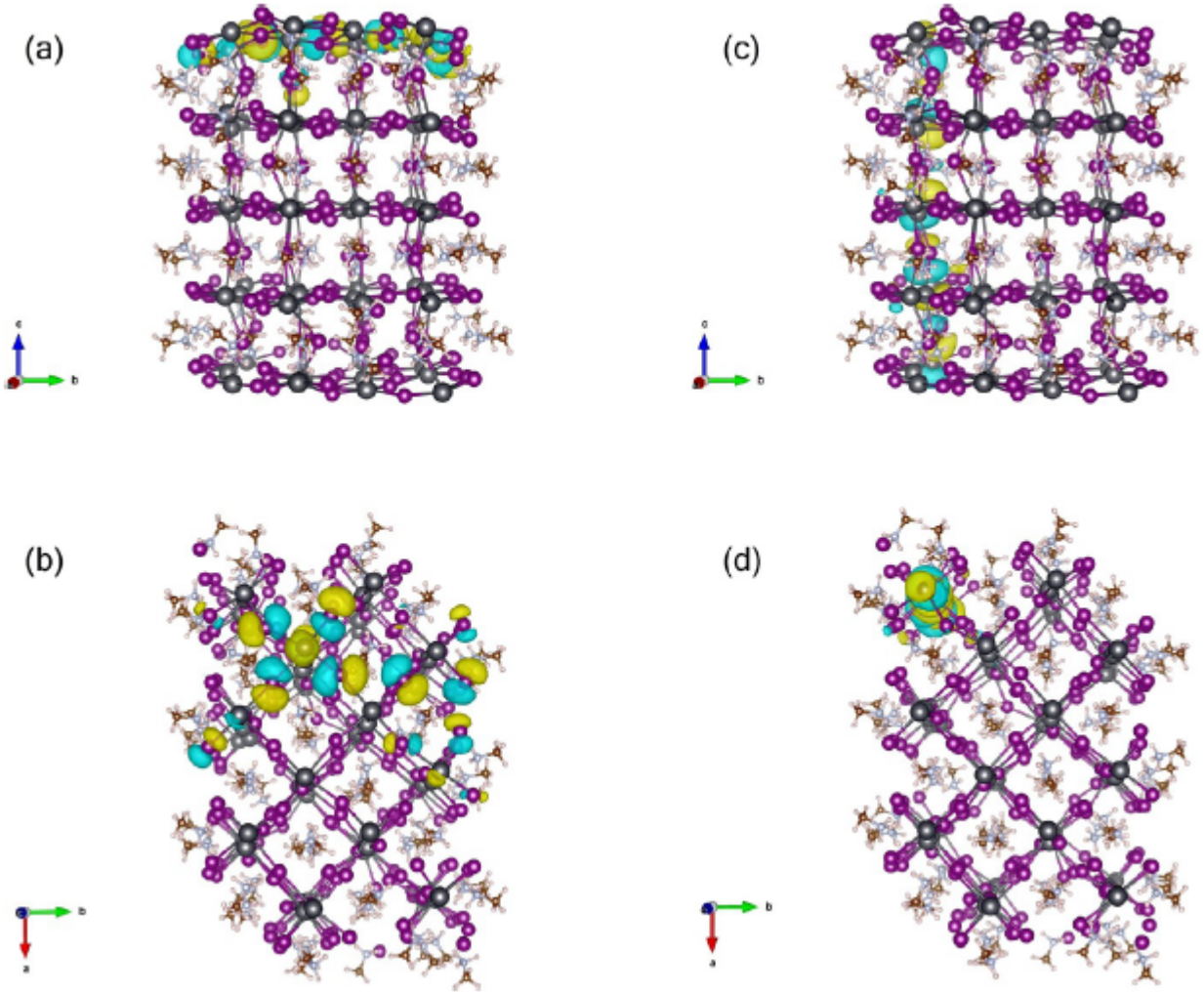

G. Giorgi, K. Yamashita, *J. Phys. Chem. Lett.*, **7**, 888-899 (2016)

(a) Lateral and (b) top view of VBM (after 1.90 ps, 1.73 eV);
(c) and (d) the same views for CBM

Rotational Timescale

Rotational autocorrelation function $c(\Delta t)$:

$$c(\Delta t) = \frac{1}{N_{\text{cations}}} \sum_i \langle \mathbf{s}_i(t) \cdot \mathbf{s}_i(t + \Delta t) \rangle$$

where i and si(t) are the index of organic cations and unit vector aligned with the orientation of i-th organic cation, respectively.

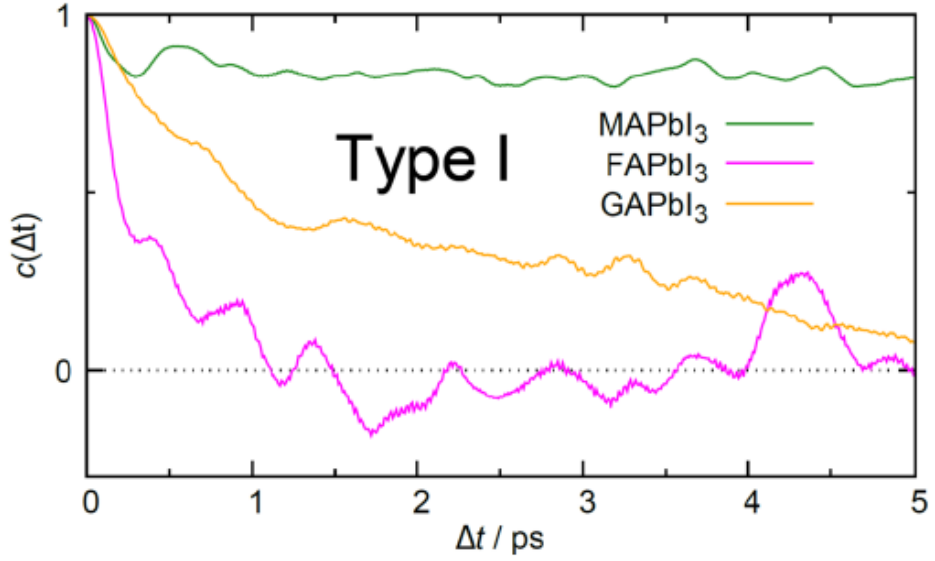

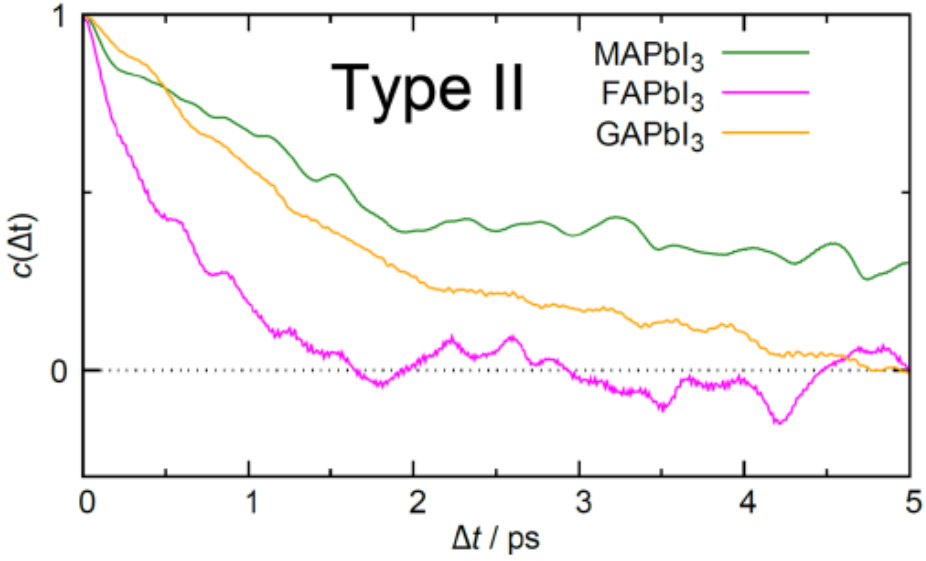

H. Uratani, K. Yamashita, submitted (2017)

Charge Separation

Overlap integral q:

$$q = \int_{V_{\mathrm{cell}}} |\psi_{\mathrm{VBM}}(\mathbf{r})||\psi_{\mathrm{CBM}}(\mathbf{r})|d\mathbf{r} = \int_{V_{\mathrm{cell}}} \sqrt{\rho_{\mathrm{VBM}}(\mathbf{r})\rho_{\mathrm{CBM}}(\mathbf{r})}d\mathbf{r}$$

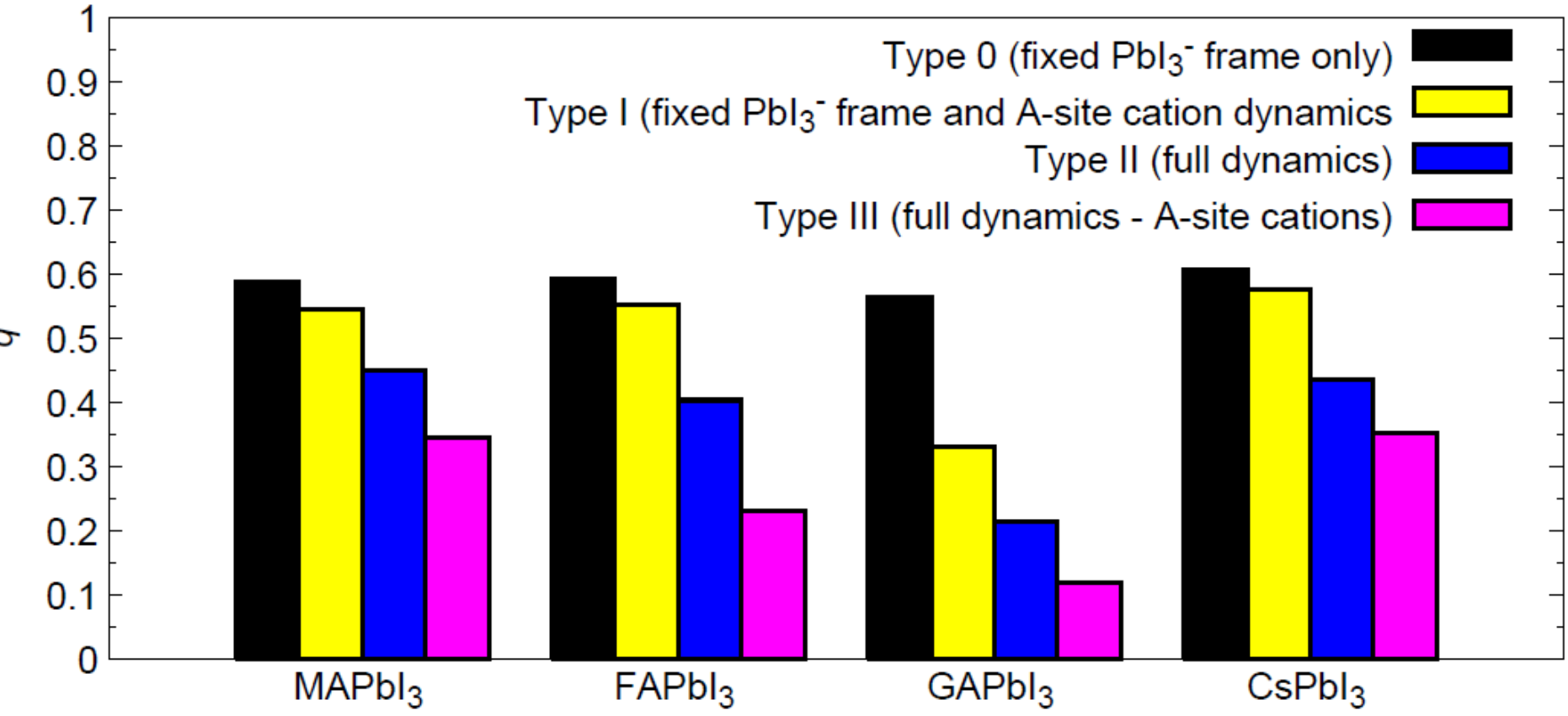

H. Uratani, K. Yamashita, submitted (2017)

Summary

High performance of lead halide perovskite-based photovoltaic devices

Remarkable carrier properties

- Long carrier diffusion length
- long carrier lifetime
- low electron-hole recombination rate

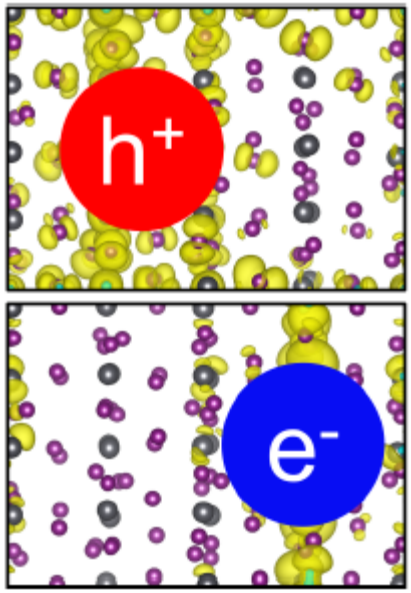

First-principles molecular dynamics simulations

the charge separation is induced by the structural fluctuation of the inorganic lattice

the charge separation is attributed to the electrostatic potential fluctuation coupled to the inorganic lattice dynamics

the organic cations are unlikely to be essential for carrier properties.

Acknowledgements

Prof. Giacomo Giorgi
The University of Perugia

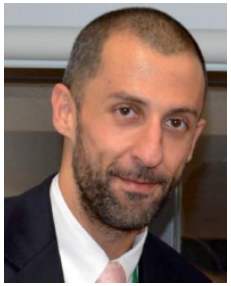

Dr. Hiroki Kawai

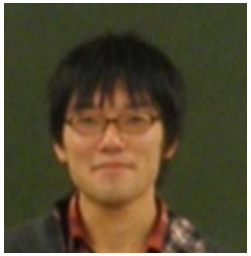

Theoretical Chemistry Lab.
The University of Tokyo

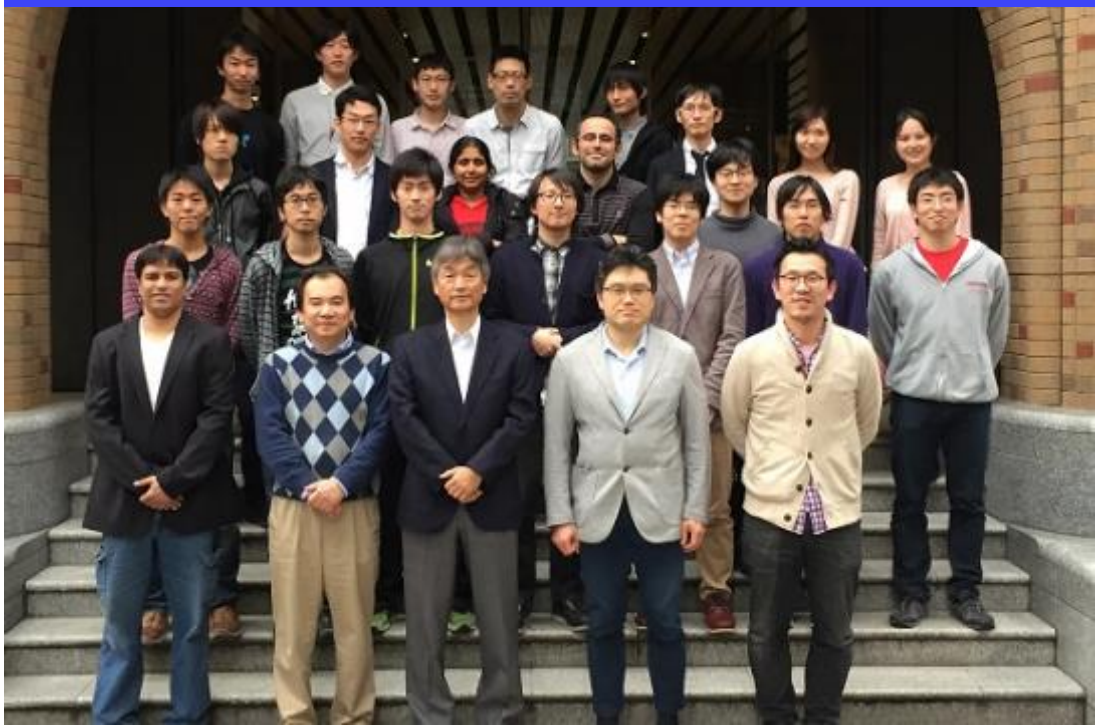

Mr. Hiroki Uratani

CREST

Prof. Andrea Marini (ETSF, Italy)

FIRST Project
Prof. Hiroshi Segawa
(UT, RCAST)

$Cs_{54}Pb_{27}I_{108}$ cluster

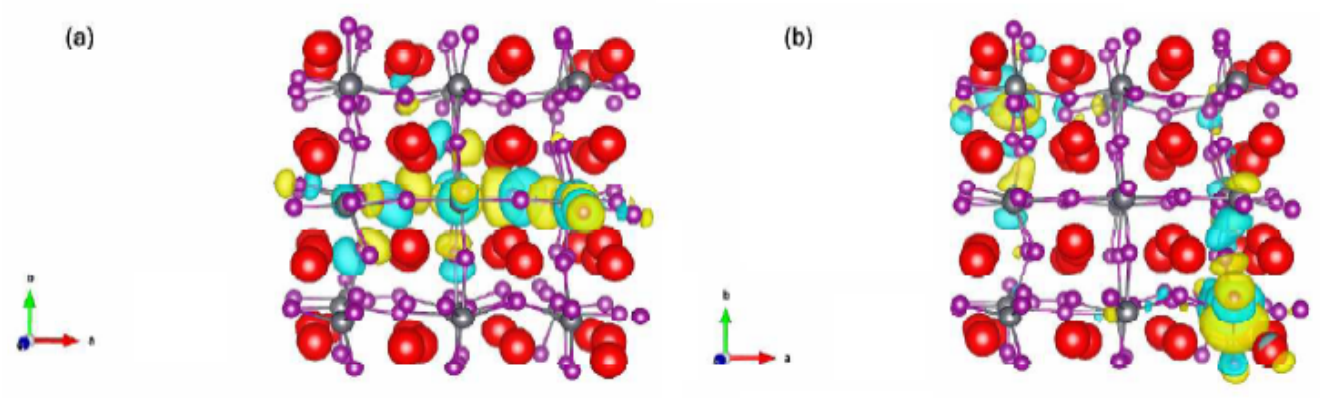

Top view of (a) VBM and (b) CBM (Gray, Pb; purple, I; red, Cs)

The localization of the wave function is more spread out and symmetrically distributed over the whole cluster as a consequence of the replacement of the A-site cation.

The comparison with inorganic halide perovskites supports the idea that the dipole and the rotation of the organic cation play a primary role in the localization of the wave function in $MAPbI_3$ clusters.

The charge localization causes electron-hole separation and reduces carrier recombination rates.

G. Giorgi, K. Yamashita, *J. Phys. Chem. Lett.*, **7**, 888-899 (2016)

Summary

A) The effective masses of photogenerated electrons and holes were estimated to be $m_e^* = 0.23m_0$ and $m_h^* = 0.29m_0$, respectively, including spin−orbit coupling effects. This result is consistent with the long-range ambipolar transport property and with the larger diffusion constant for carriers.

B) A newly developed MBPT method is applied to analyze the carrier relaxation lifetime of $MAPbI_3$ perovskites.

C) Halide Perovskites other than $CH_3NH_3PbI_3$ are suggested featuring
(1) zero dipole moment Guanidium cations,
(2) aliovalent ionic pairs replace Pb cations.

D) We have introduced and discussed the properties of zero dimensional (clusters) of organic−inorganic halide perovskites. The present study represents the first analysis focused on the electronic and structural properties of OIHP clusters.

E) The dipole and the rotation of the organic cation play a primary role in the localization of the wave function in $MAPbI_3$ clusters. **The charge localization causes electron-hole separation and reduces carrier recombination rates.**

Review articles: G. Giorgi, K. Yamashita, *J. Mater. Chem. A*, **3**, 8981-8991 (2015)

G. Giorgi, K. Yamashita, *Nanotechnology*, in press (2015)

ab initio Molecular Dynamics

AIMD simulations
- DFT GGA/PBE
- NVE ensemble
- Siesta code

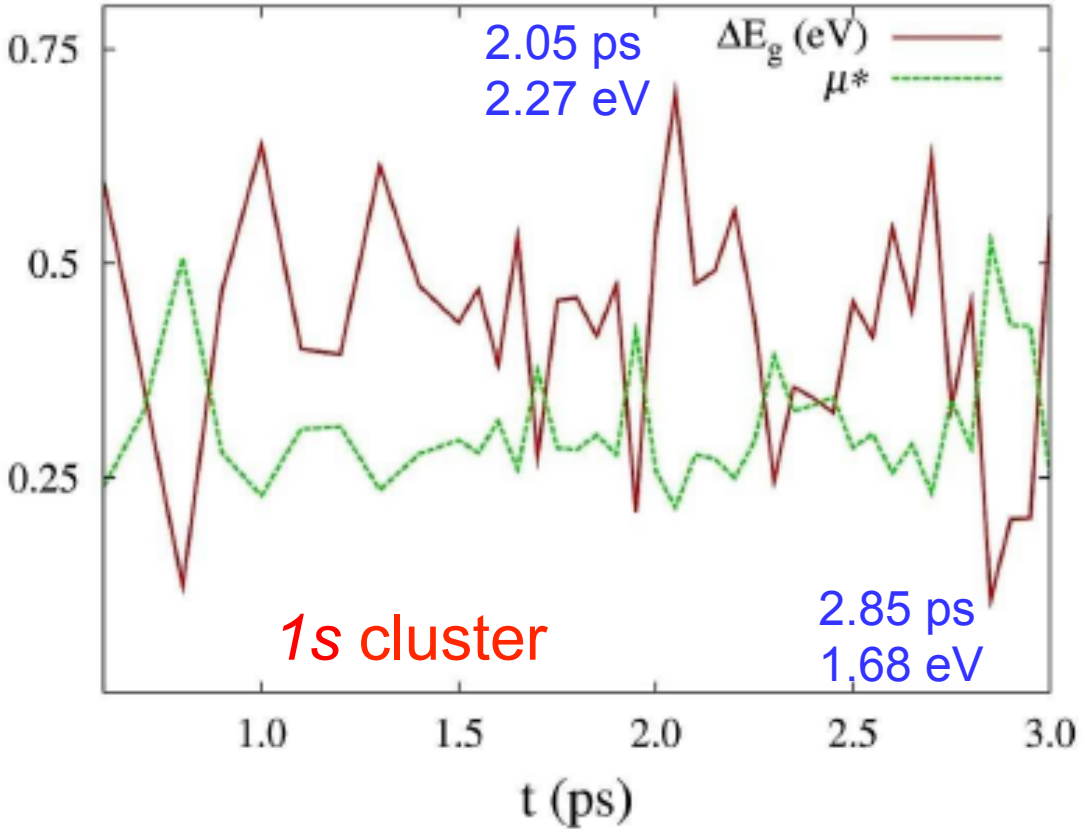

Brus's equation (1986);

$$\Delta E_g \approx (2h^2\pi^2/\mu D^2) - (3.6e^2/\varepsilon D)$$

$1/\mu = 1/m_e^* + 1/m_h^*$ $\quad D = (6V/\pi)^{1/3}$

G. Giorgi, K. Yamashita, *J. Phys. Chem. Lett.*, **7**, 888-899 (2016)

DOS evolution of *1s* cluster

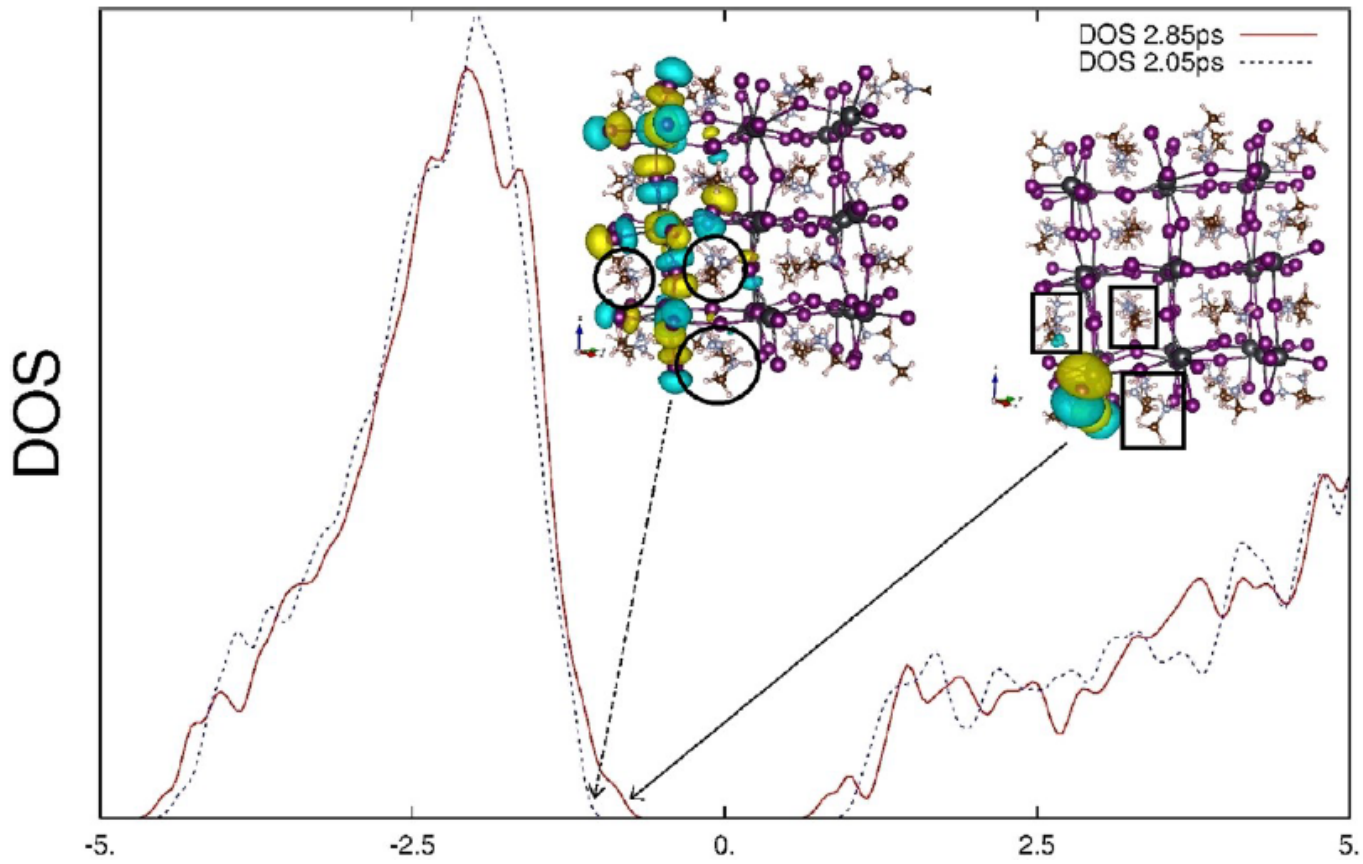

The coherent/random orientation of the MA cations thus seems to play a role on the wave function localization preferential sites at the surface.

G. Giorgi, K. Yamashita, *J. Phys. Chem. Lett.*, **7**, 888-899(2016)

Hot-Hole Cooling

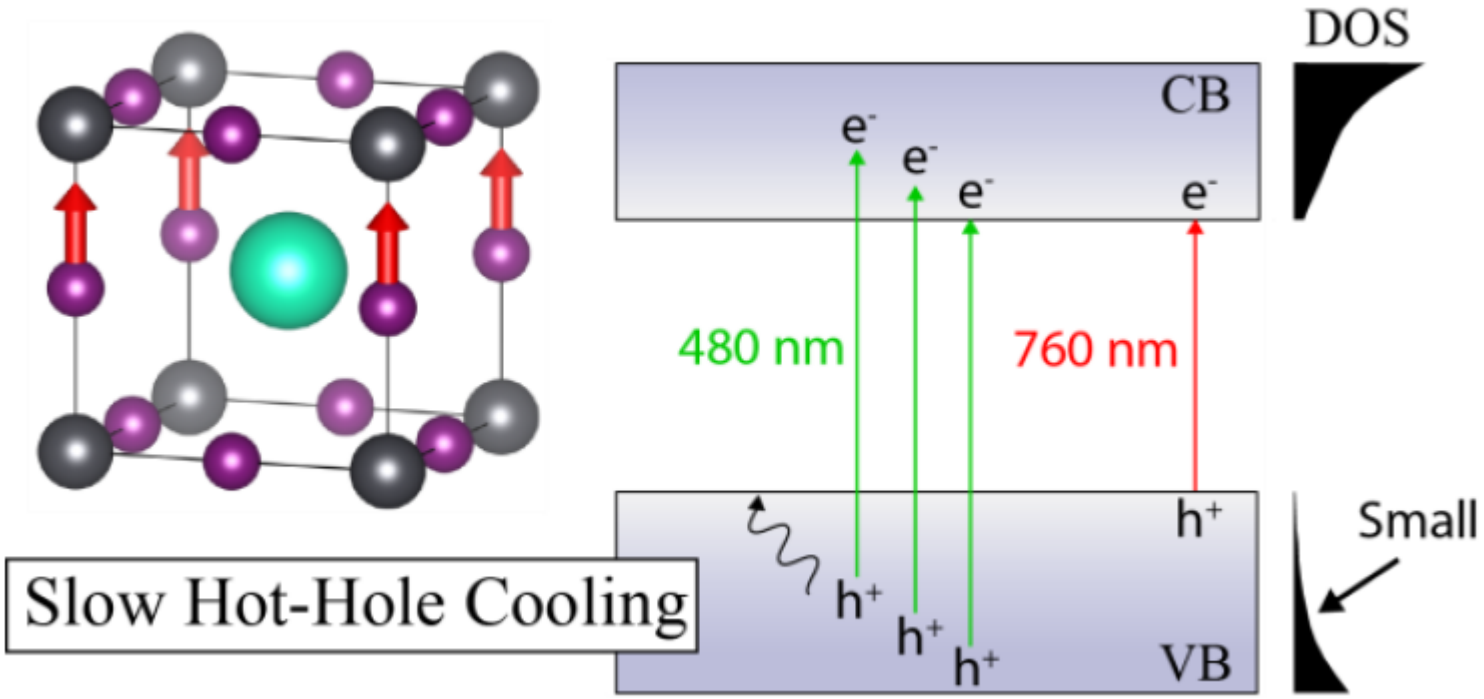

■ A reduction of the relaxation paths in the small valence DOS as being the origin of the slow hot-hole cooling.

■ The 480-nm peak can be assigned to transitions from the VB states along the R-M path.

H. Kawai, G.Giorgi, A. Marini, K. Yamashita, *Nano Lett., 15, 3103-3108* (2015)

Dual nature of excited states

Stamplecoskie, Manser, Kamat, Energy Environ. Sci. **8**, 208(2015)

Excited state behavior of PbI_x^{n-} complex in solution

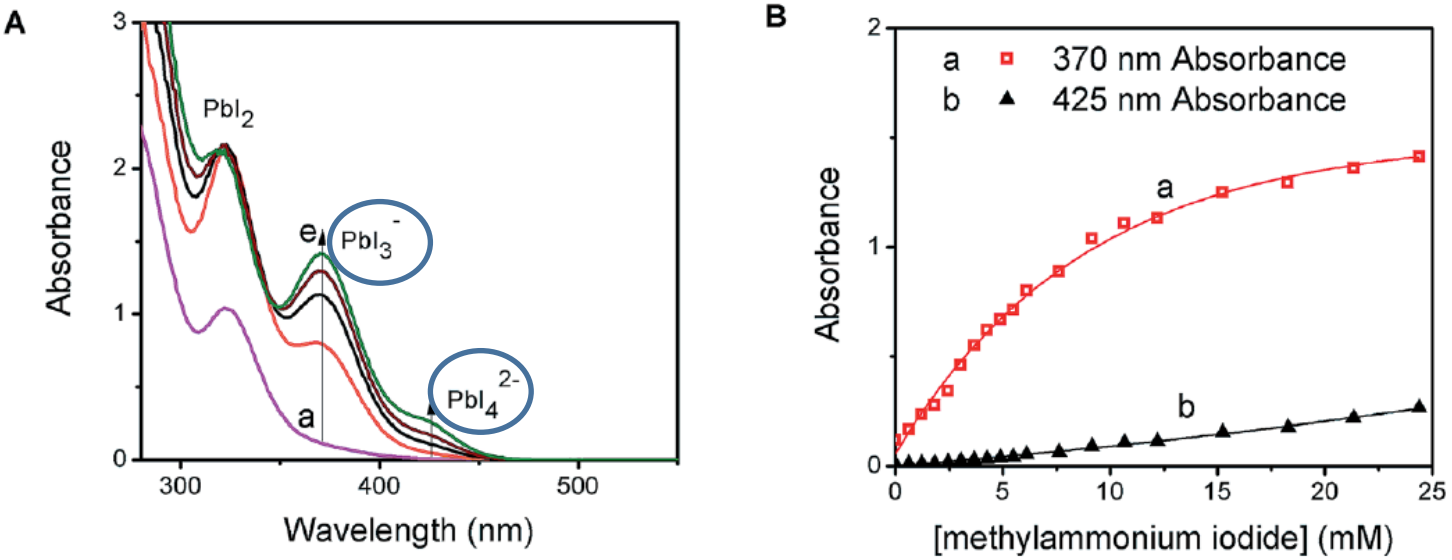

Absorption spectra of 250 μM PbI_2 solution in dimethylformamide (a) with increasing concentration of MAI from 6mM(b) to 24mM(e)

Excited state behavior of perovskite films

760nm

$$CH_3NH_3PbI_3 + h\nu \rightarrow CH_3NH_3PbI_3\,[h + e] \rightarrow CH_3NH_3PbI_3$$

480nm $\quad CH_3NH_3PbI_3 + h\nu \rightarrow [CH_3NH_3PbI\cdots I_2]$

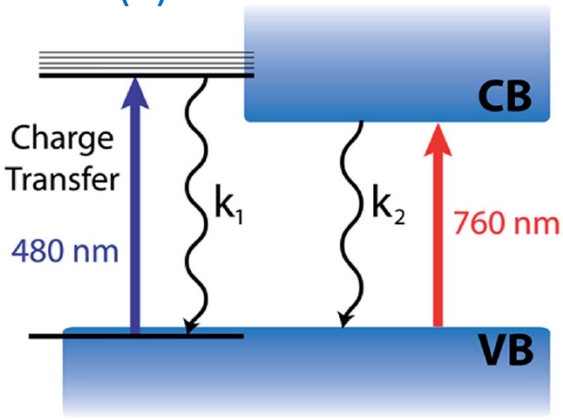

MA_4PbI_6, $MA_7Pb_2I_{11}$ Clusters

B3LYP/6-311G++,MWB46(halides), MWB78(Pb)

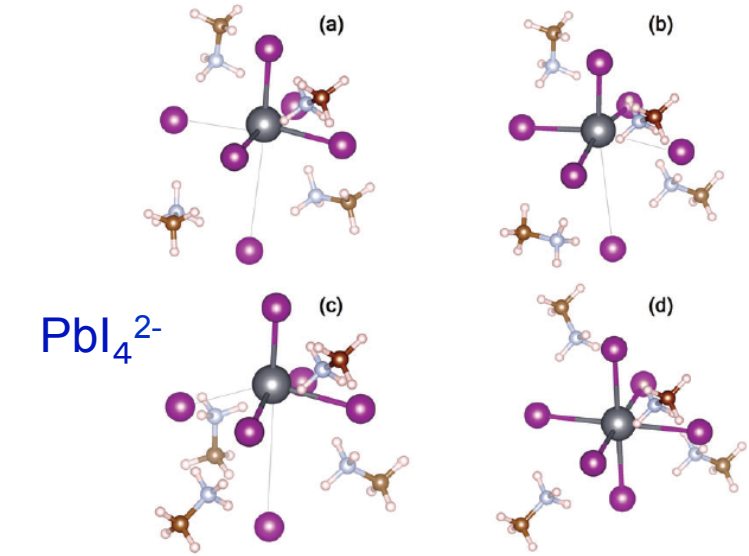

PbI_4^{2-}

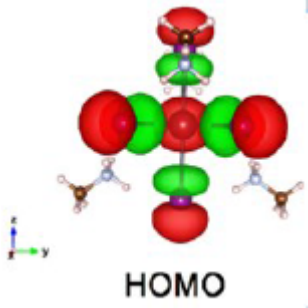

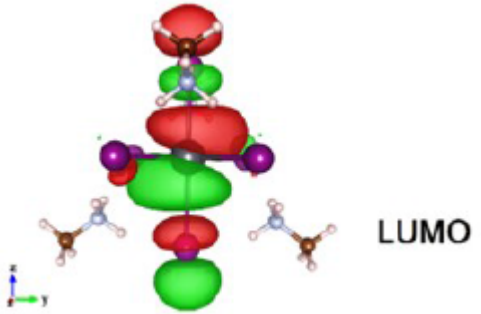

MA_4PbI_6

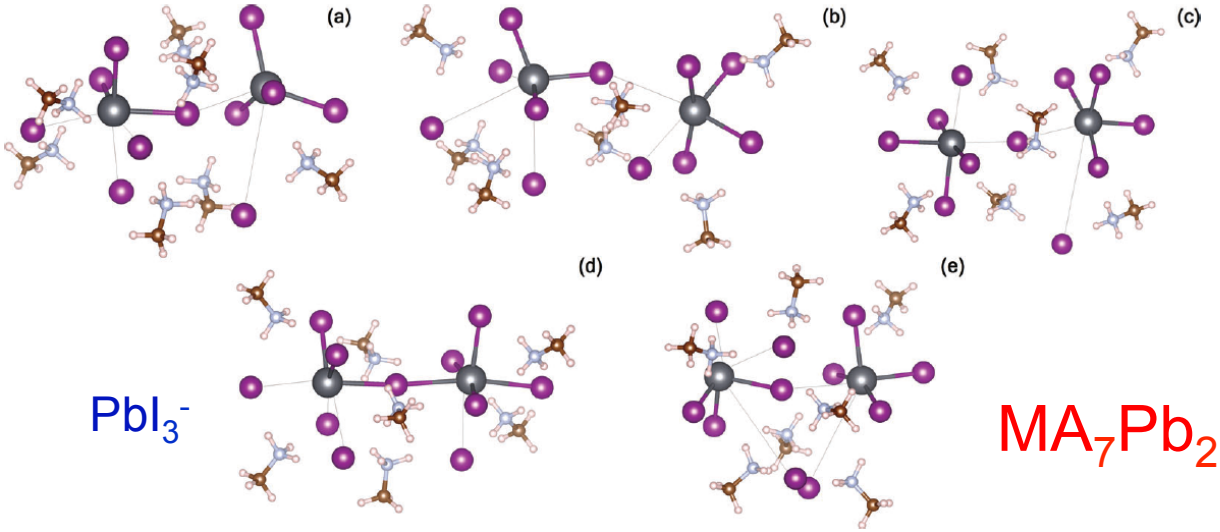

PbI_3^-

$MA_7Pb_2I_{11}$

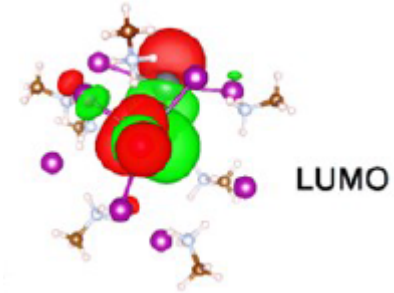

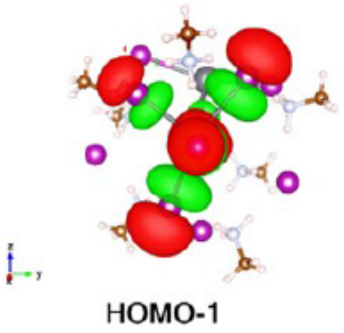

G. Giorgi, T. Yoshihara, K. Yamashita, *PCCP*, **18**, 21092 (2016)

Relationship between EDM and FMO

FMO overlap integral

$$S = \int \mathbf{dr} |\psi_{\mathrm{HOMO}}||\psi_{\mathrm{LUMO}}|$$

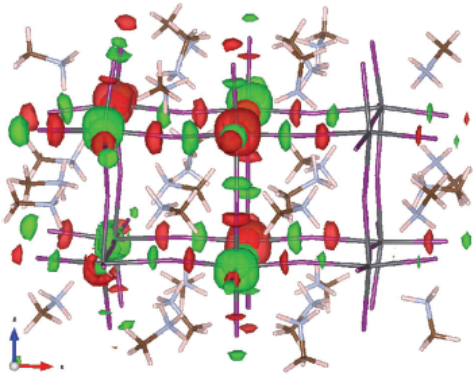

HOMO

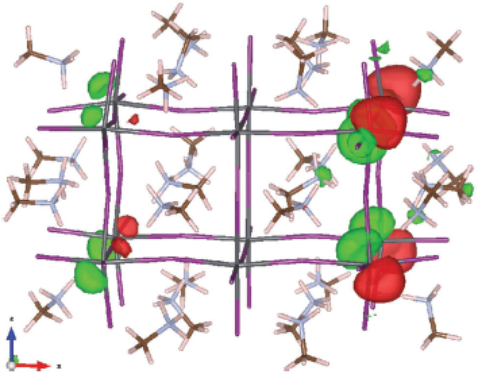

LUMO

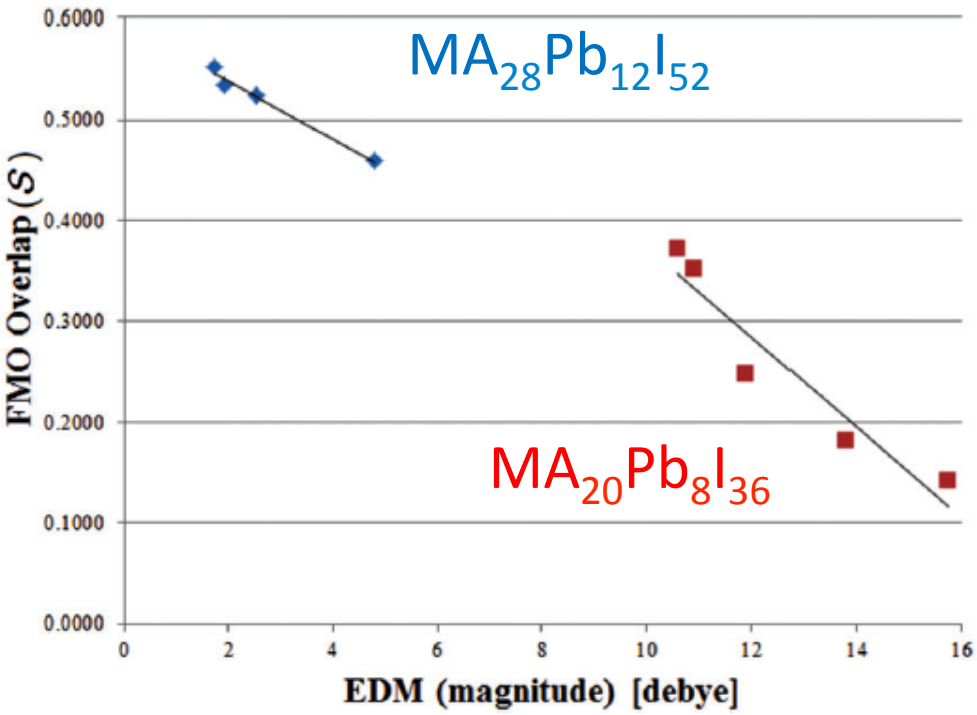

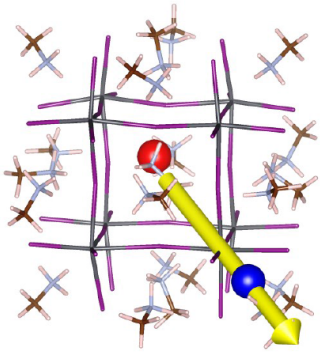

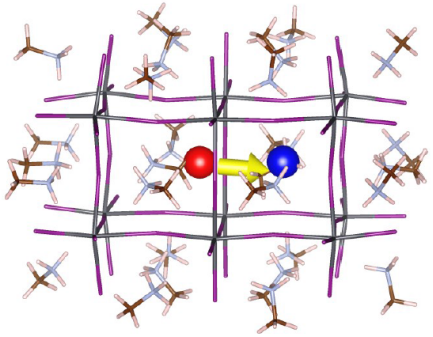

G. Giorgi, T. Yoshihara, K. Yamashita, *PCCP*, **18**, 21092 (2016)

Poster Presentation

Mr. Hiroki Uratani

4669 Charge Carrier Trapping at Surface Defects of Perovskite Solar Cell Absorbers: A First-Principles Study

Hiroki Uratani, Koichi Yamashita

J. Phys. Chem. Lett. January 27 (2017)

ACS Editor's Choice Selection

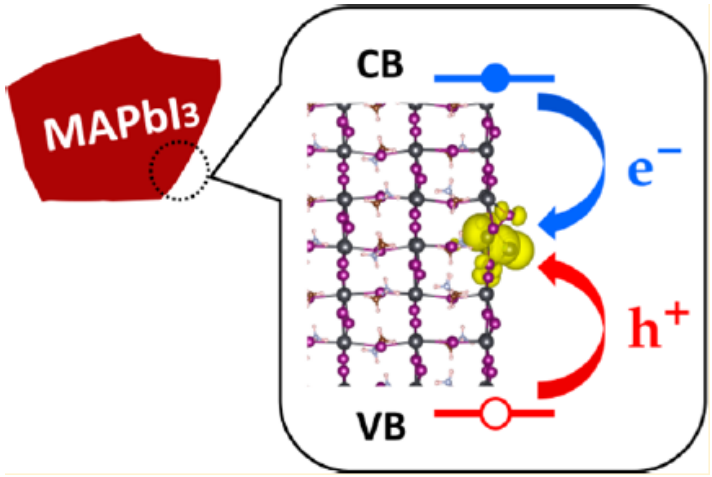

Nanostructured OIHPs

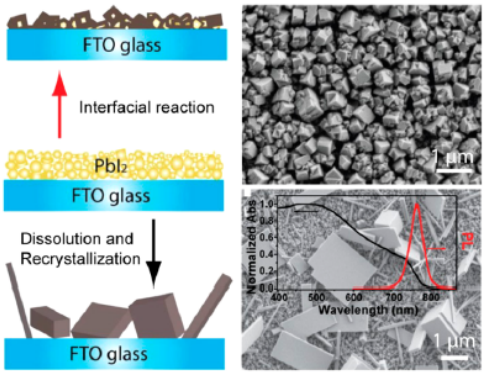

Nanowires, nanorods, nanoplates

Long carrier lifetime

Fu, Jin et al.

J. Am. Chem. Soc. 2015

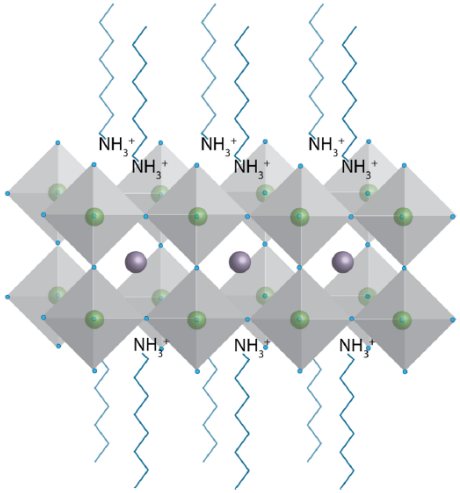

Colloidal Nanoplates

Sharp excitonic absorption

Tyagi, Arveson, Tisdale

J. Phys. Chem. Lett. 2015

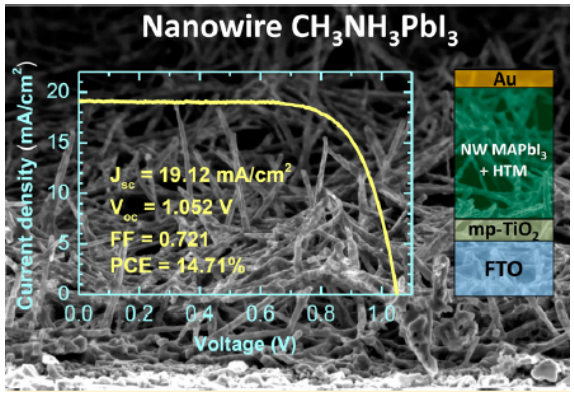

Nanowire

Enhanced excitonic nature

Im, Grätzel, Park et al.

Nano Lett. 2015

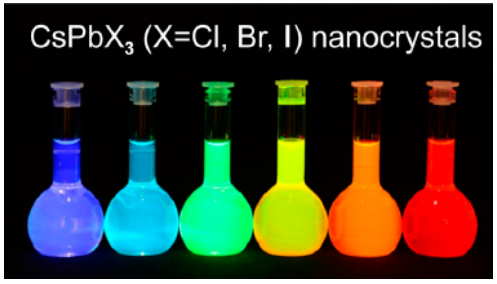

Nanocrystals

Bandgap tunability

Protesescu, Kovalenko et al.

Nano Lett. 2015

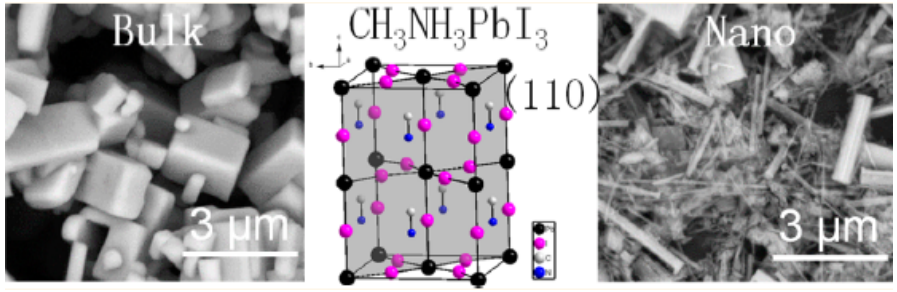

Nanocrystals

Long photoluminescence times

Zhu, Petrich, Smith, Vela et al.

ACS Nano 2015

Ion Migration in Organometal Trihalide Perovskite and Its Impact on Photovoltaic Efficiency and Stability

Yongbo Yuan and Jinsong Huang, *Acc. Chem. Res.*, **49**, 528 (2016)

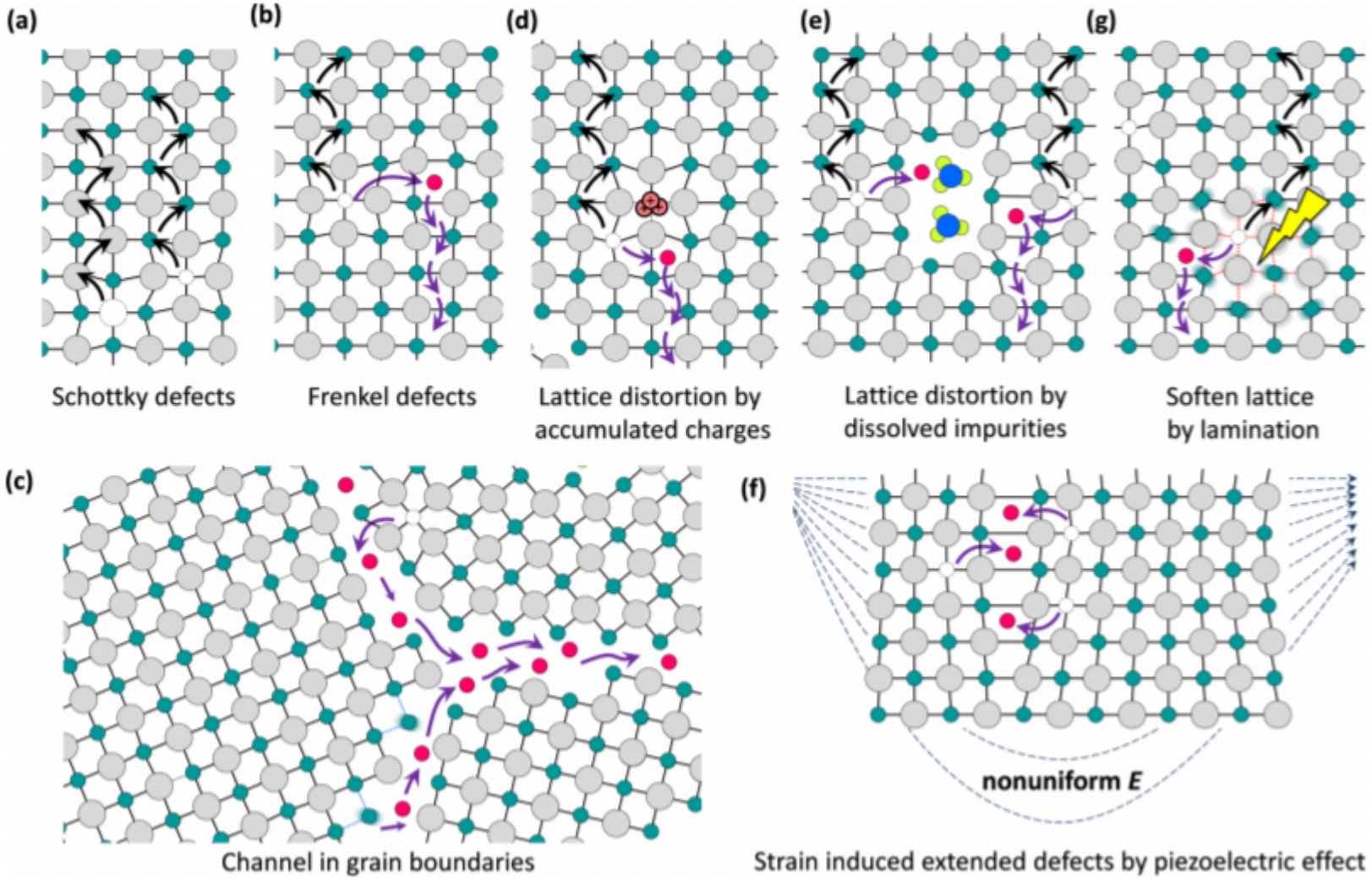

Long Electron-Hole Diffusion Lengths

Ambipolar charge transfer

- Absorber (Kim *et al*. 2012, Heo *et al*. 2013)
  TiO_2/$MAPbI_3$/HTM
- Electron transporter (Lee *et al.* 2012)
  Al_2O_3/$MAPbI_3$/HTM
- Hole transporter (Etgar *et al.* 2012)
  without HTM

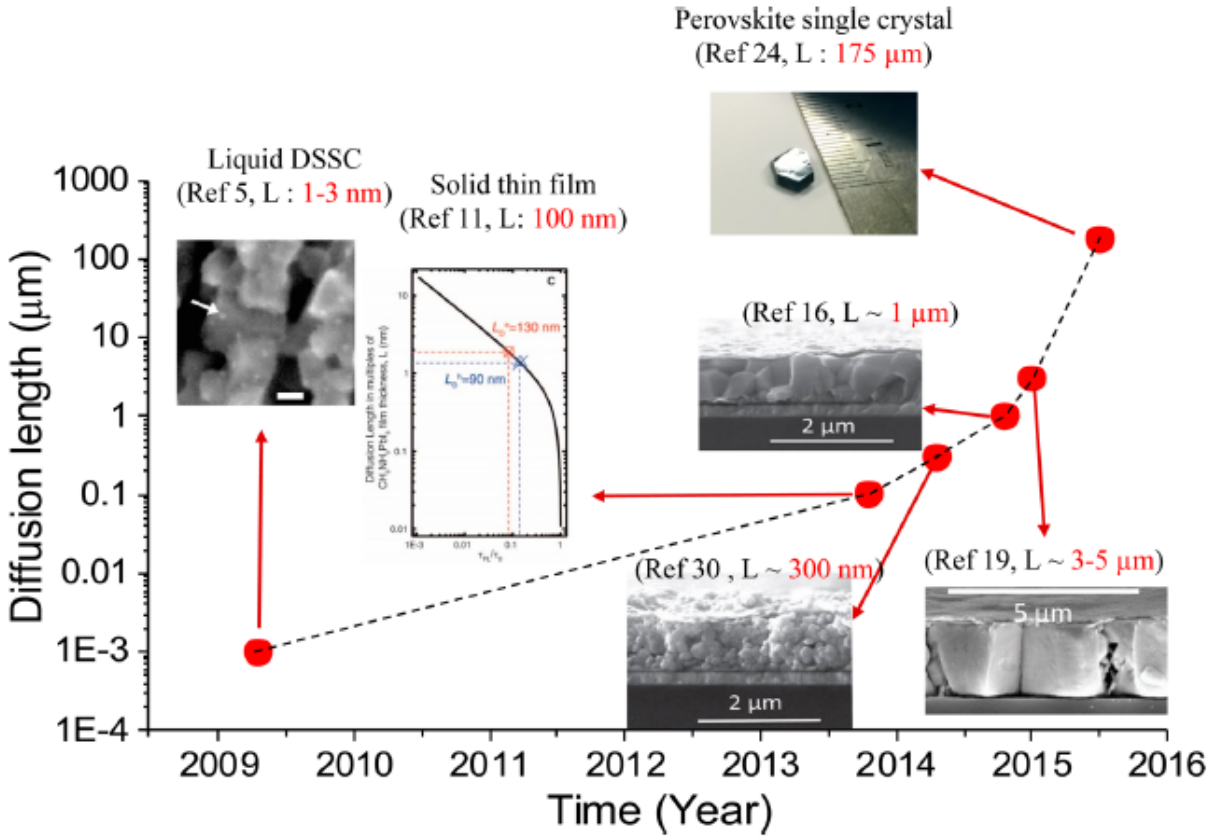

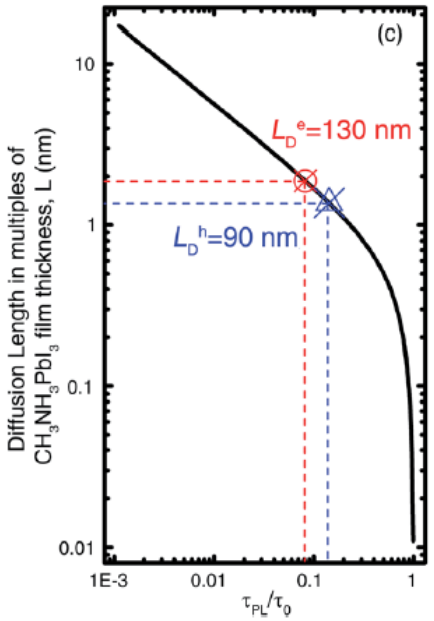

Xing *et al.*, Science (2013)

$MAPbI_{3-x}Cl_x$, >1 μm,
Stranks et al. Science (2013)

Huang et al. JPCL (2015)

Superior point defect properties

W. J. Yin, T. Shi and Y. Yan,
Appl. Phys. Lett., 2014, 104, 063903.

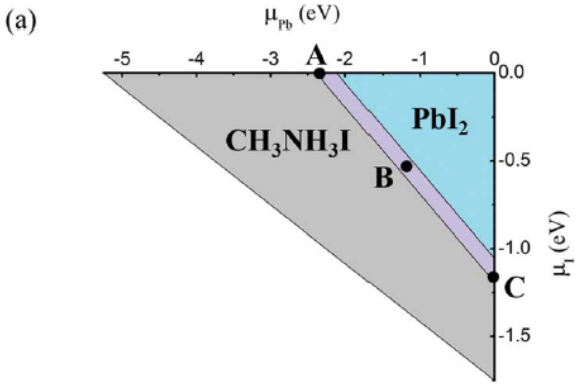

Vacancies (V_{MA}, V_{Pb}, V_I), interstitials (MA_i, Pb_i, I_i), cation substitutions (MA_{Pb}, Pb_{MA}) and antisite substitutions (MA_I, Pb_I, I_{MA}, I_{Pb})

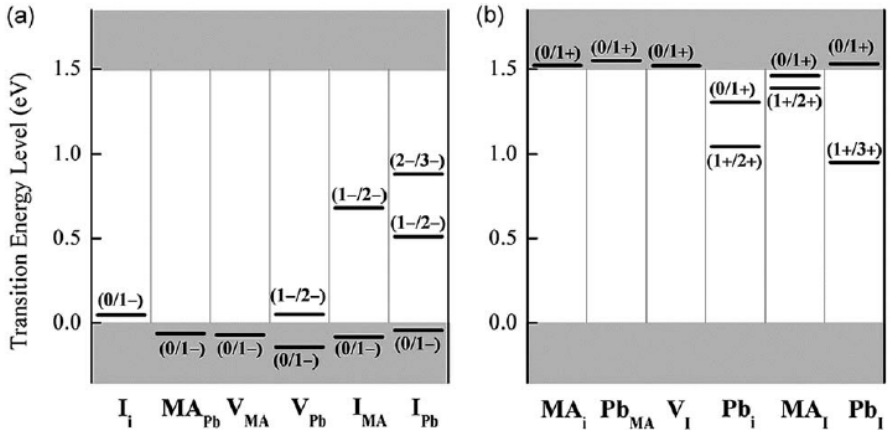

Electrically benign structural disorder

W.-J. Yin, J-H. Yang, J. Kang, Y. Yan, S.-H. Wei, J. Mater. Chem. A, 2014.

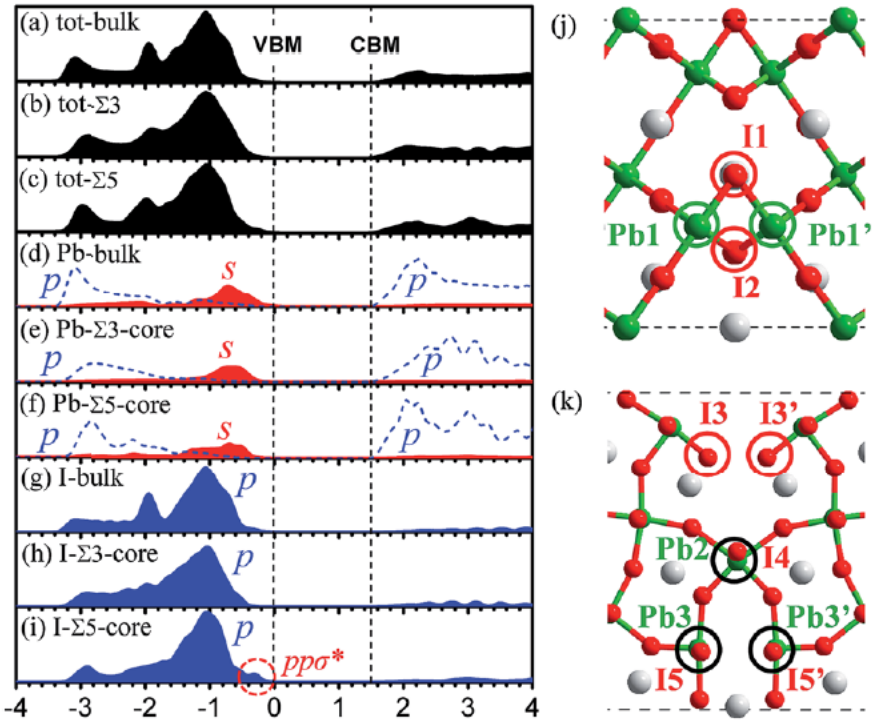

(a–i) are (partial) DOS of pristine $CsPbI_3$ and polycrystalline $CsPbI_3$ with Σ3(111) and Σ5(310) GBs. (j) and (k) are atomic structures at Σ3(111) and Σ5(310) GBs respectively.

Halide Perovskites other than $CH_3NH_3PbI_3$ (1)

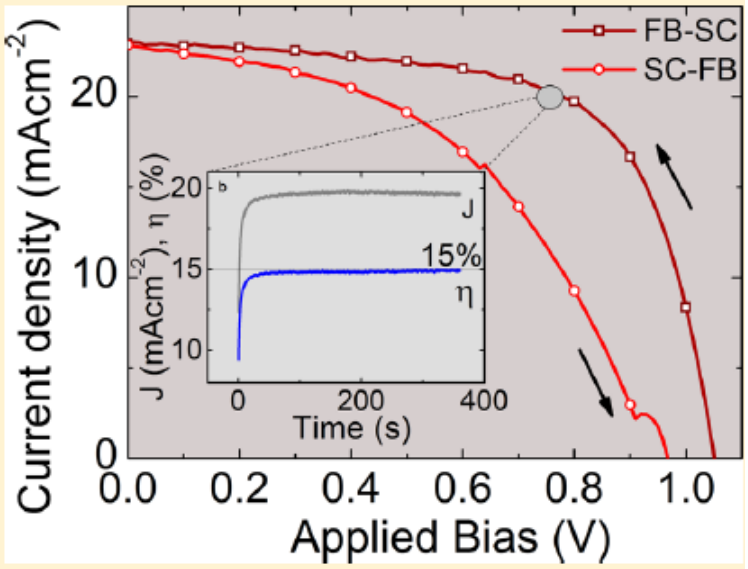

H.J. Snaith *et al*, *J. Phys. Chem. Lett.* (2014) **5**, 1511

A large hysteresis in the current-voltage curves may be attributed to the motion of organic cations with a permanent dipole moment in response to the applied electric field.

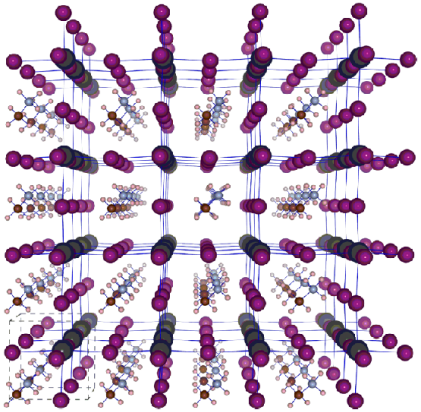

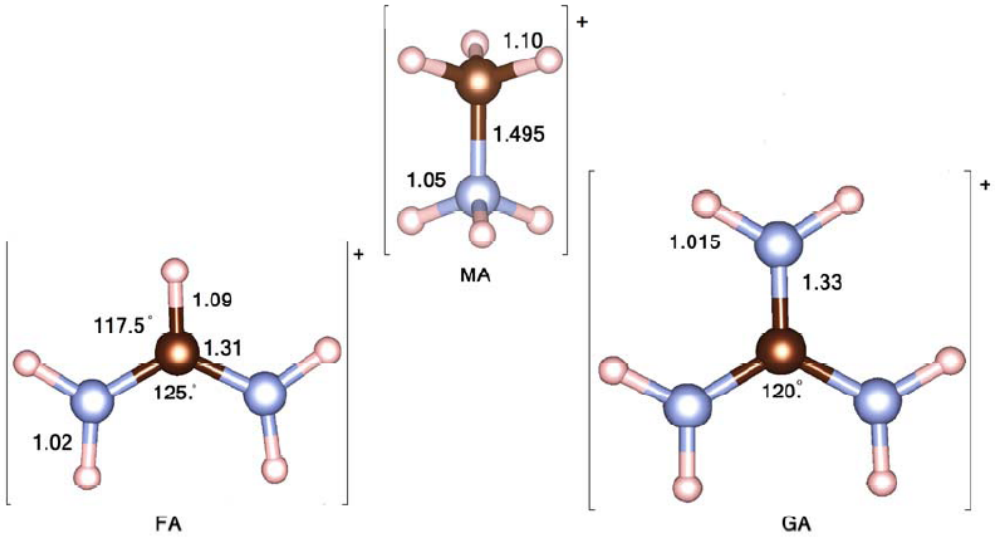

Organic cations that have a zero dipole moment and a molecular size qwell fitted to the lead iodine cavity.

Giorgi, Fujisawa, Segawa, Yamashita, J. Phys. Chem. C, 119, 4694 (2015).

Halide Perovskites other than $CH_3NH_3PbI_3$ (2)

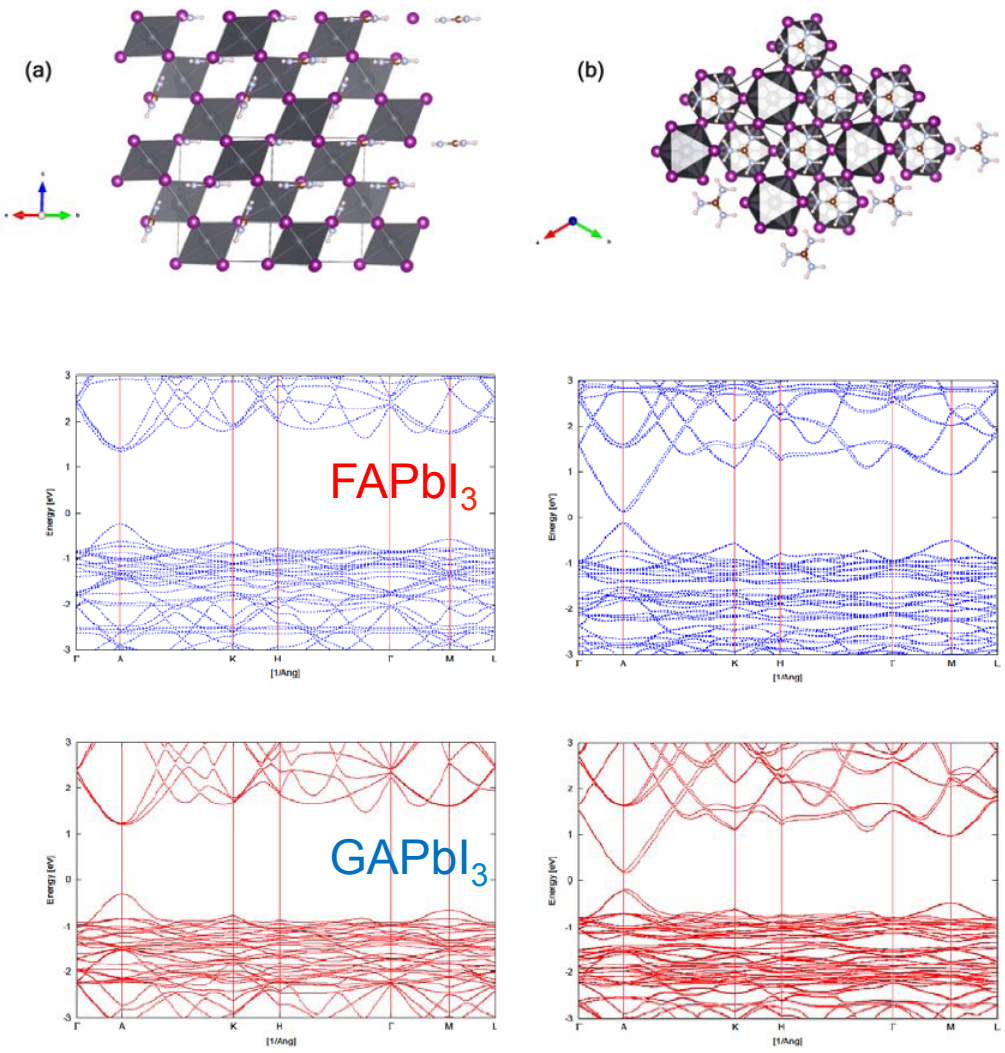

Effective mass of carriers (A-Γdirection)

$FAPbI_3$

$m_h^*=0.302\ m_0$, $m_e^*=0.403m_0$

$GAPbI_3$

$m_h^*=0.385m_0$, $m_e^*=0.359m_0$

Ratio: m_h^*/m_e^*

$FAPbI_3$ (*0.75*), $GAPbI_3$ (1.07)

$GAPbI_3$ has a more marked ambipolar behaviour than $FAPbI_3$

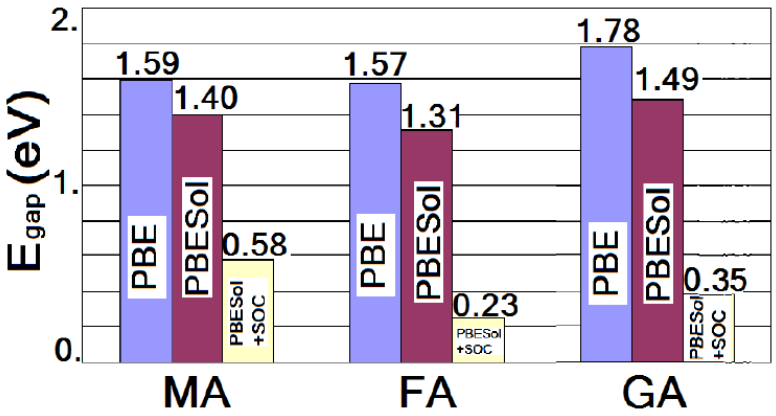

Giorgi, Fujisawa, Segawa, Yamashita, J. Phys. Chem. C, 119, 4694 (2015).

Guanidinium: A Route to Enhanced Carrier Lifetime and Open-Circuit Voltage in Hybrid Perovskite Solar Cells

Nicholas De Marco,[†,‡] Huanping Zhou,[†,‡] Qi Chen,[†,‡] Pengyu Sun,[†] Zonghao Liu,[†,‡] Lei Meng,[†] En-Ping Yao,[†] Yongsheng Liu,[†,‡] Andy Schiffer,[‡] and Yang Yang*[,†,‡]

Nano Lett. 2016, 16, 1009−1016

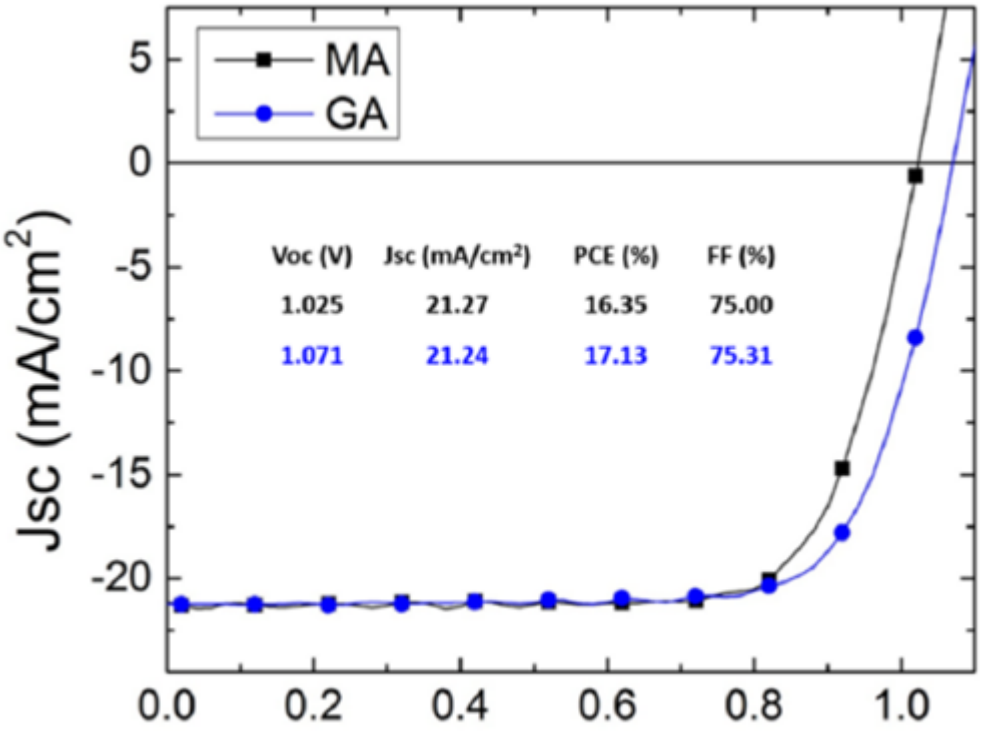

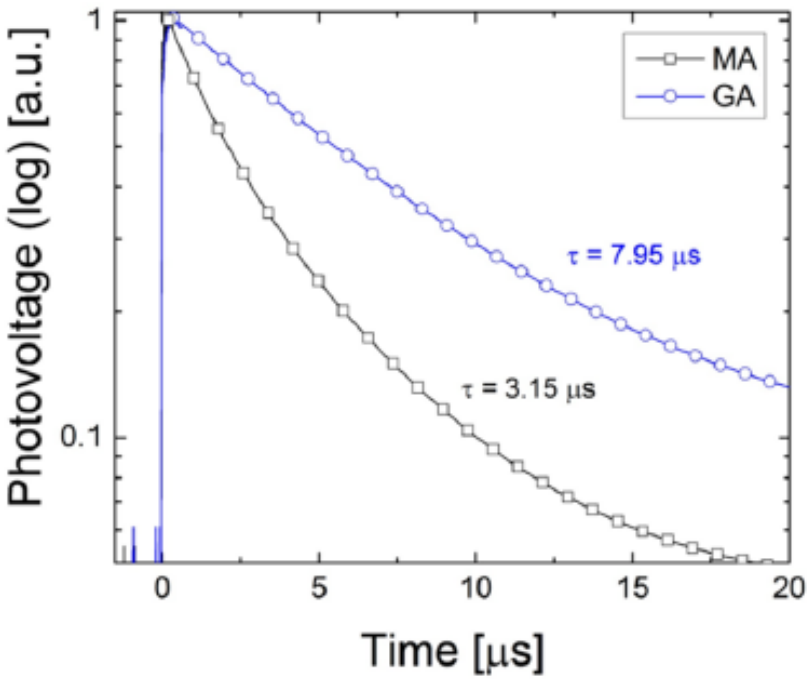

We speculate that guanidinium ions serve to suppress formation of iodide vacancies and passivate under-coordinated iodine species at grain boundaries and within the bulk through their hydrogen bonding capability.

These results present a simple method for suppressing nonradiative carrier loss in hybrid perovskites to further improve performances toward highly efficient solar cells.

Band Structures

$CH_3NH_3PbI_3$

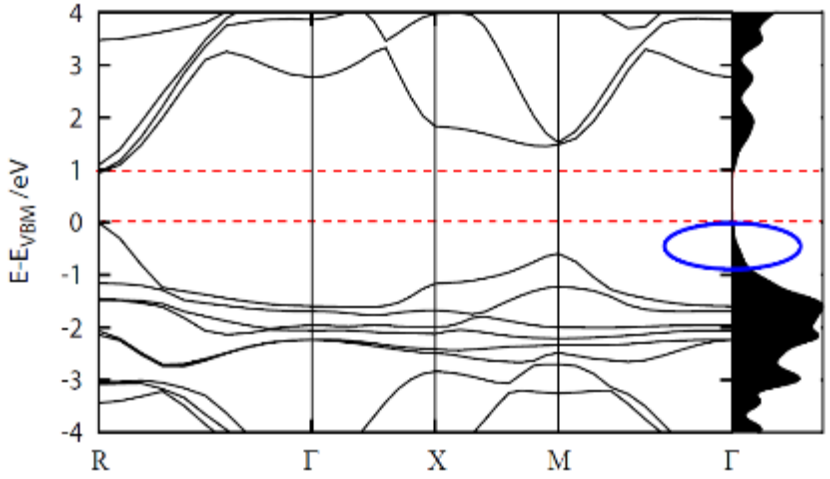

	$CH_3NH_3PbI_3$	$CsPbI_3$	PbI_3^-
Lattice constant /Å	a=c=5.99, b=6.02 ($\alpha=\gamma=86.5$, $\beta=91.0$)	6.13	6.72
Bandgap /eV	0.93	0.89	1.51

$CsPbI_3$

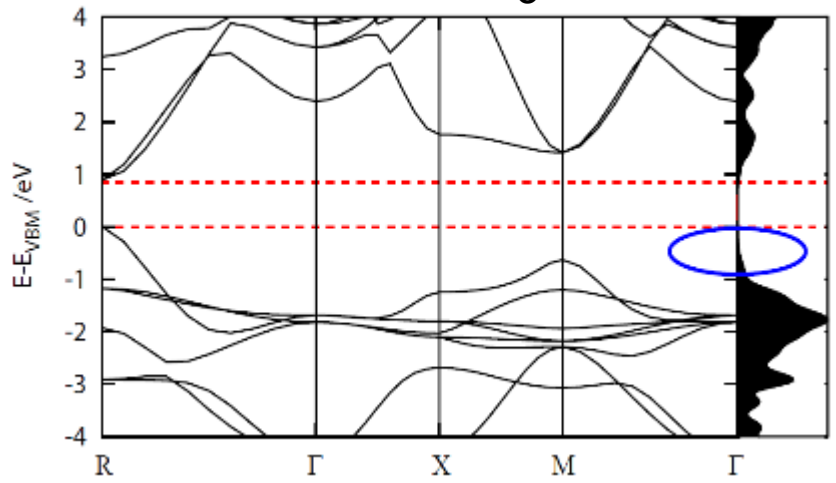

PbI_3^-

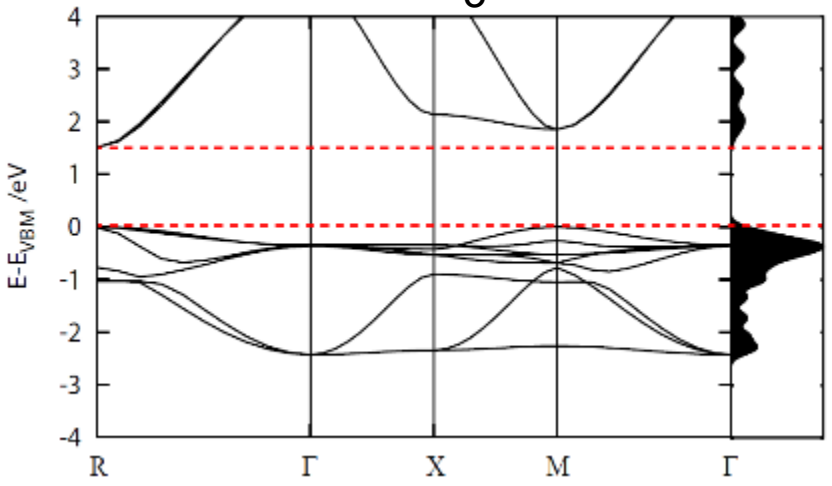

Comparison with PbI_3^-

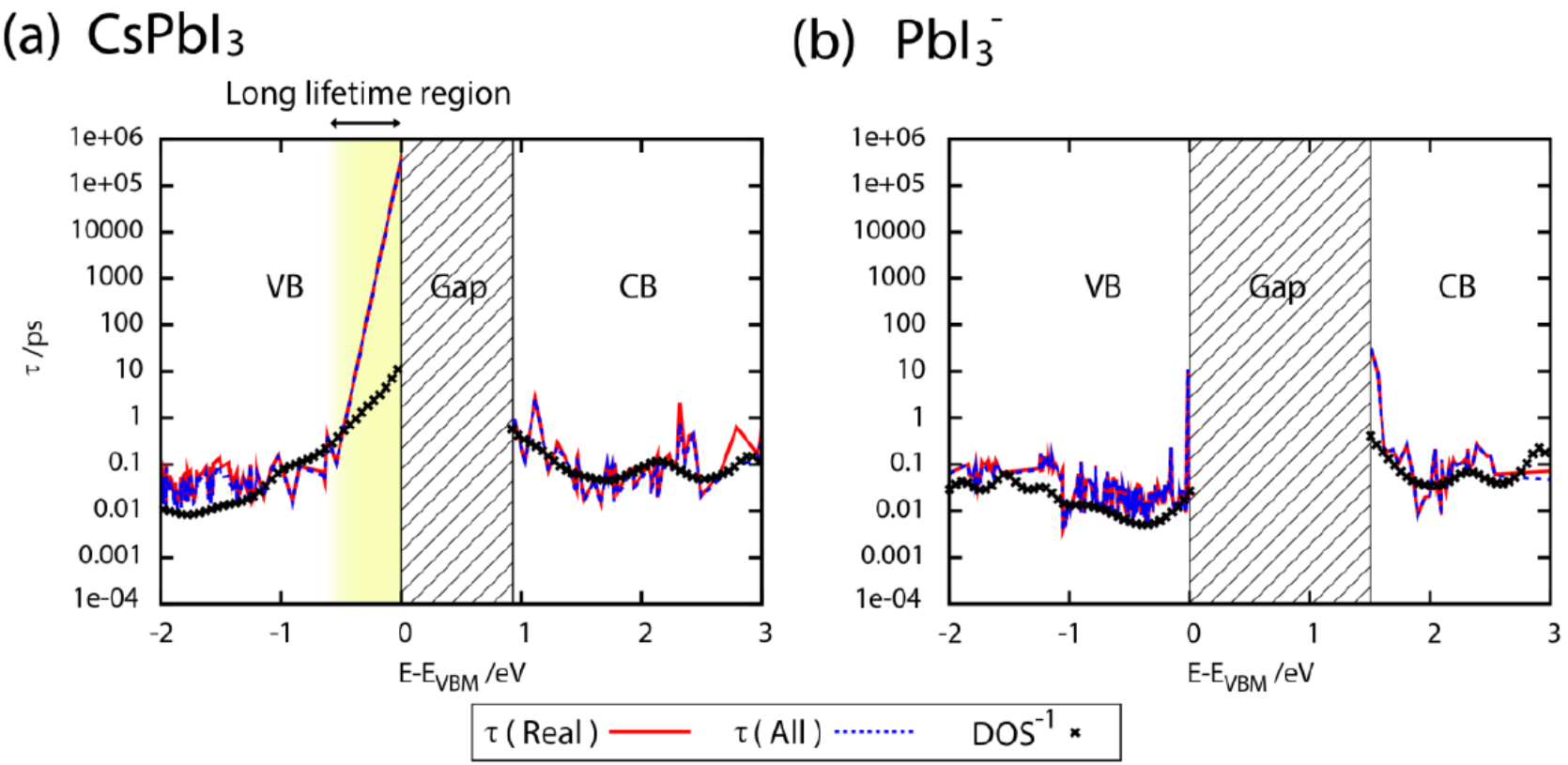

Only $CsPbI_3$ has long lifetime region of holes.

Long lifetime comes from the small DOS.

H. Kawai, G.Giorgi, A. Marini, K. Yamashita, *Nano Lett., 15, 3103-3108* (2015)

Generalized Eliashberg Function

Phonon modes contributing to the carrier relaxation

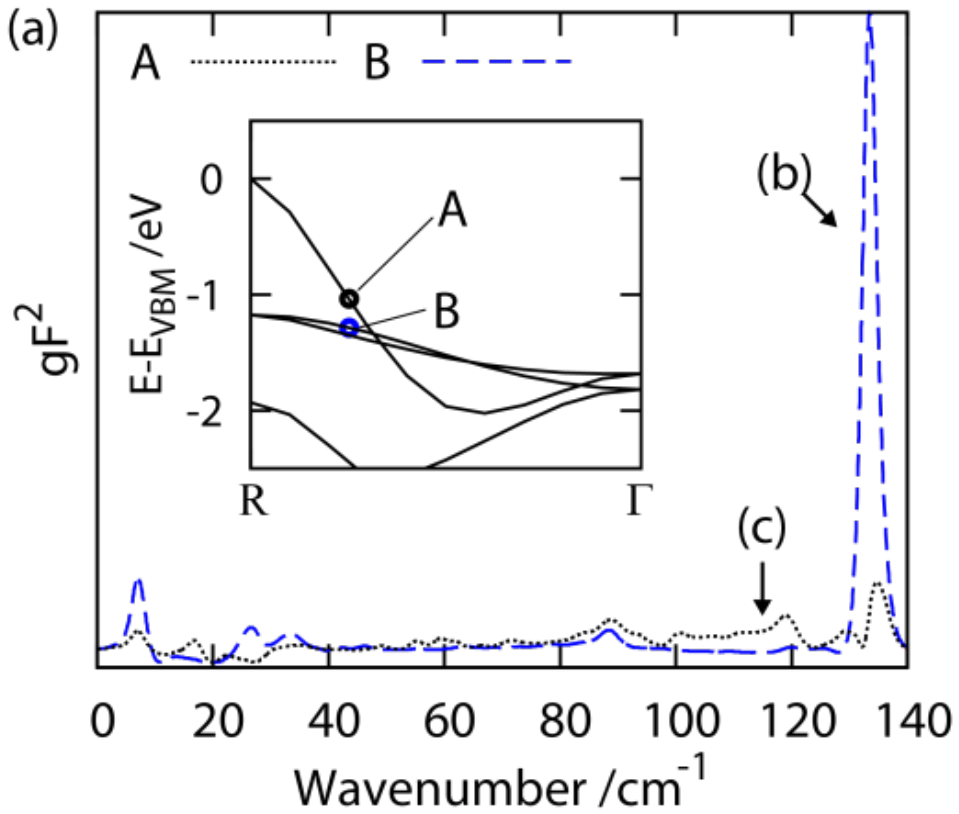

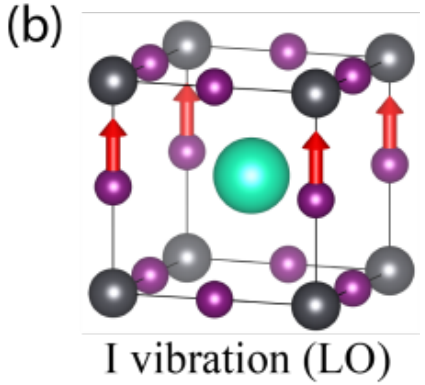

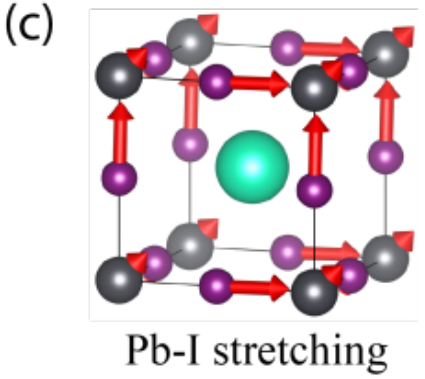

Holes are decayed through the motions of Pb and I, not Cs.

Difference of A-site cation does not alter the decay mechanism.

H. Kawai, G.Giorgi, A. Marini, K. Yamashita, *Nano Lett., 15, 3103-3108* (2015)

Optical Excitations

Optical strengths of the transitions

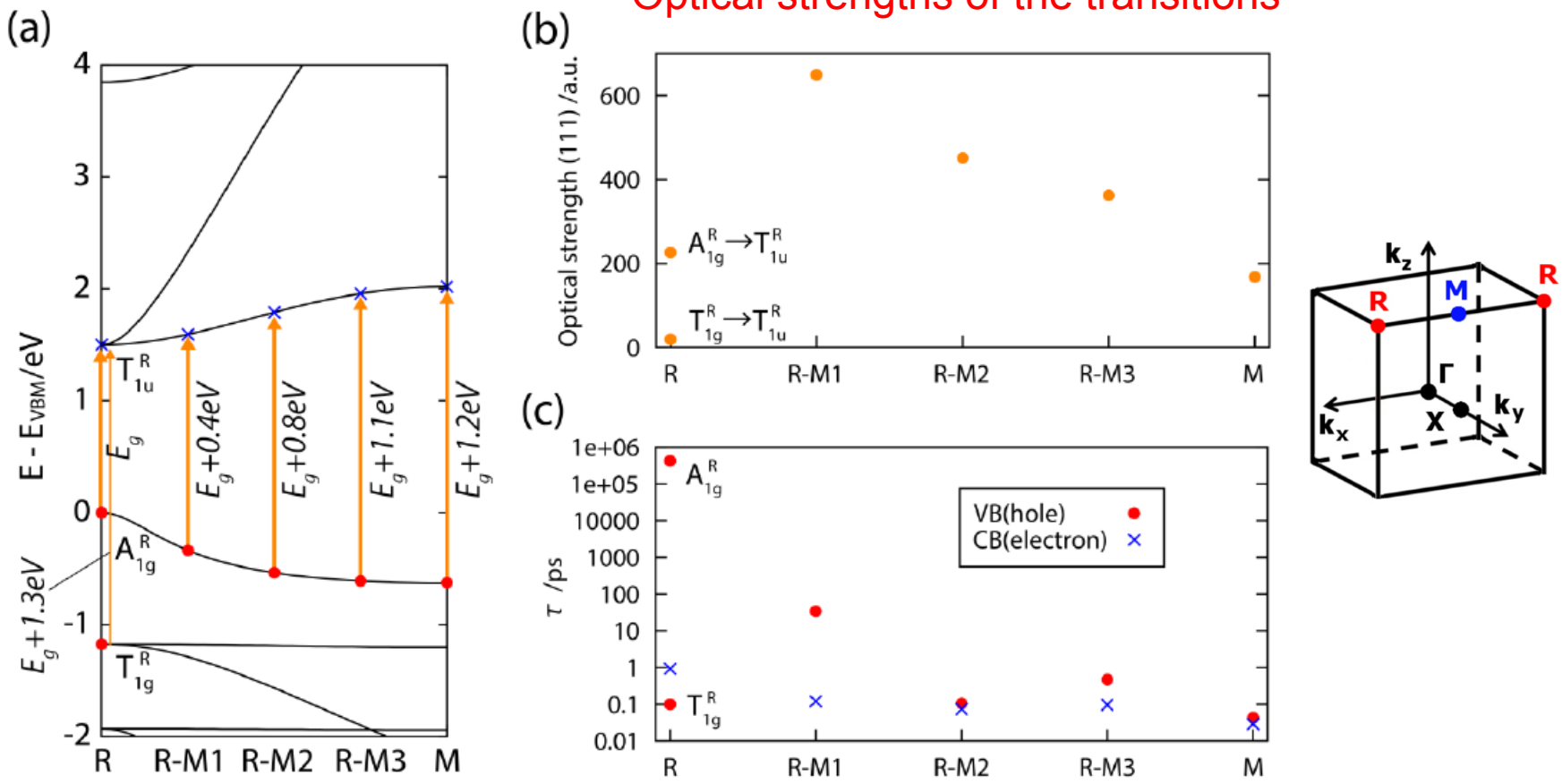

Electronic band structure of $CsPbI_3$ along the R-M path.

Carrier lifetimes at the electronic states

H. Kawai, G.Giorgi, A. Marini, K. Yamashita, *Nano Lett.*, ***15***, *3103-3108* (2015)

Bulk t-$MAPbI_3$

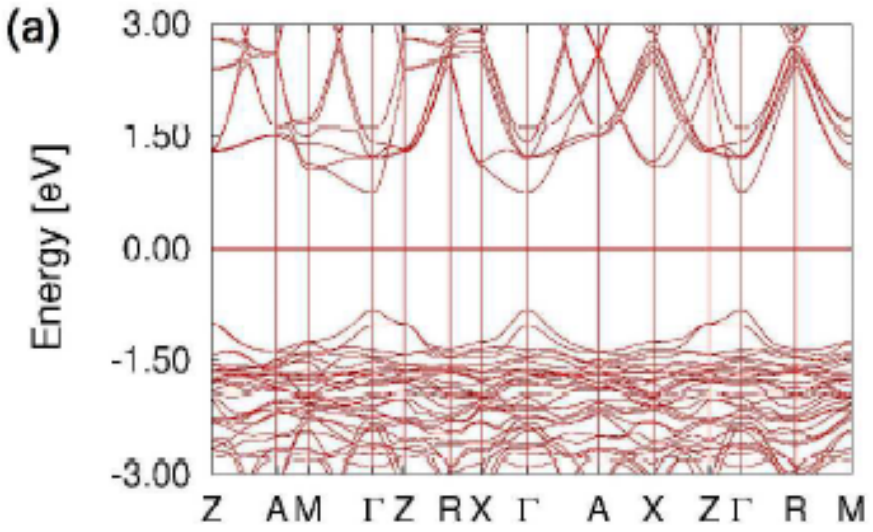

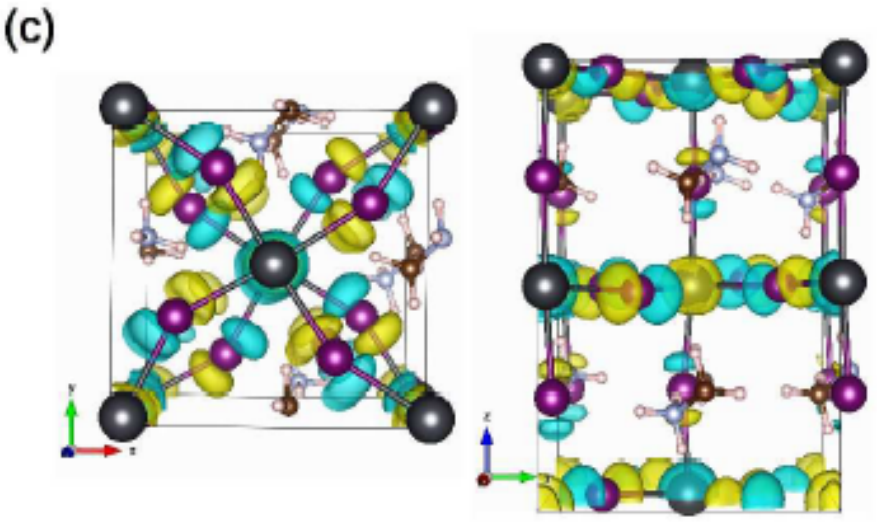

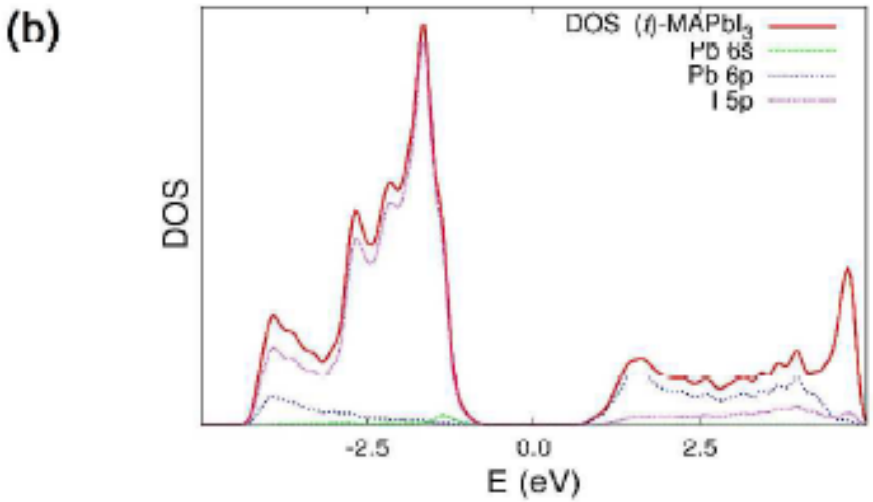

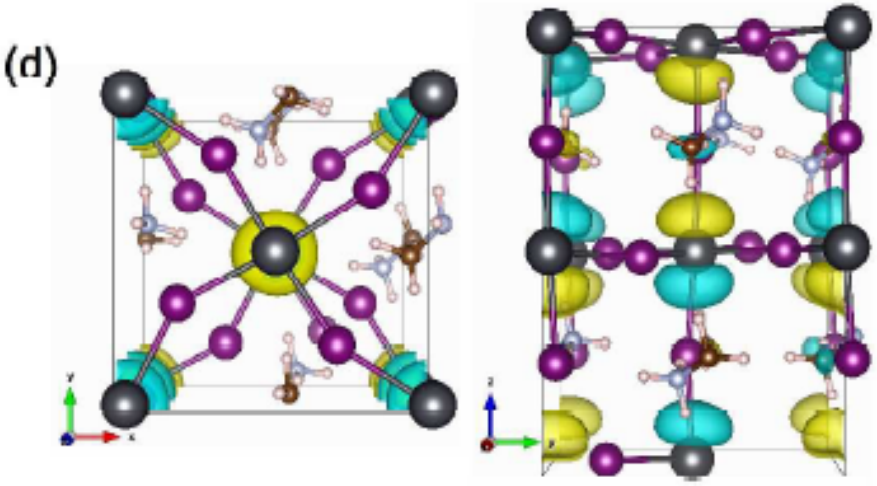

(a) PAO/PBE band structure, (b) DOS/PDOS (E_g=1.57 eV at Γ)
(c) Lateral and top view of VBM, (d) CBM

Photon recycling in lead iodide perovskite solar cells

Science **351** 1430 (2016)

Luis M. Pazos-Outón,[1] Monika Szumilo,[1] Robin Lamboll,[1*] Johannes M. Richter,[1*] Micaela Crespo-Quesada,[2] Mojtaba Abdi-Jalebi,[1] Harry J. Beeson,[1] Milan Vrućinić,[1] Mejd Alsari,[1] Henry J. Snaith,[3] Bruno Ehrler,[4] Richard H. Friend,[1†] Felix Deschler[1†]

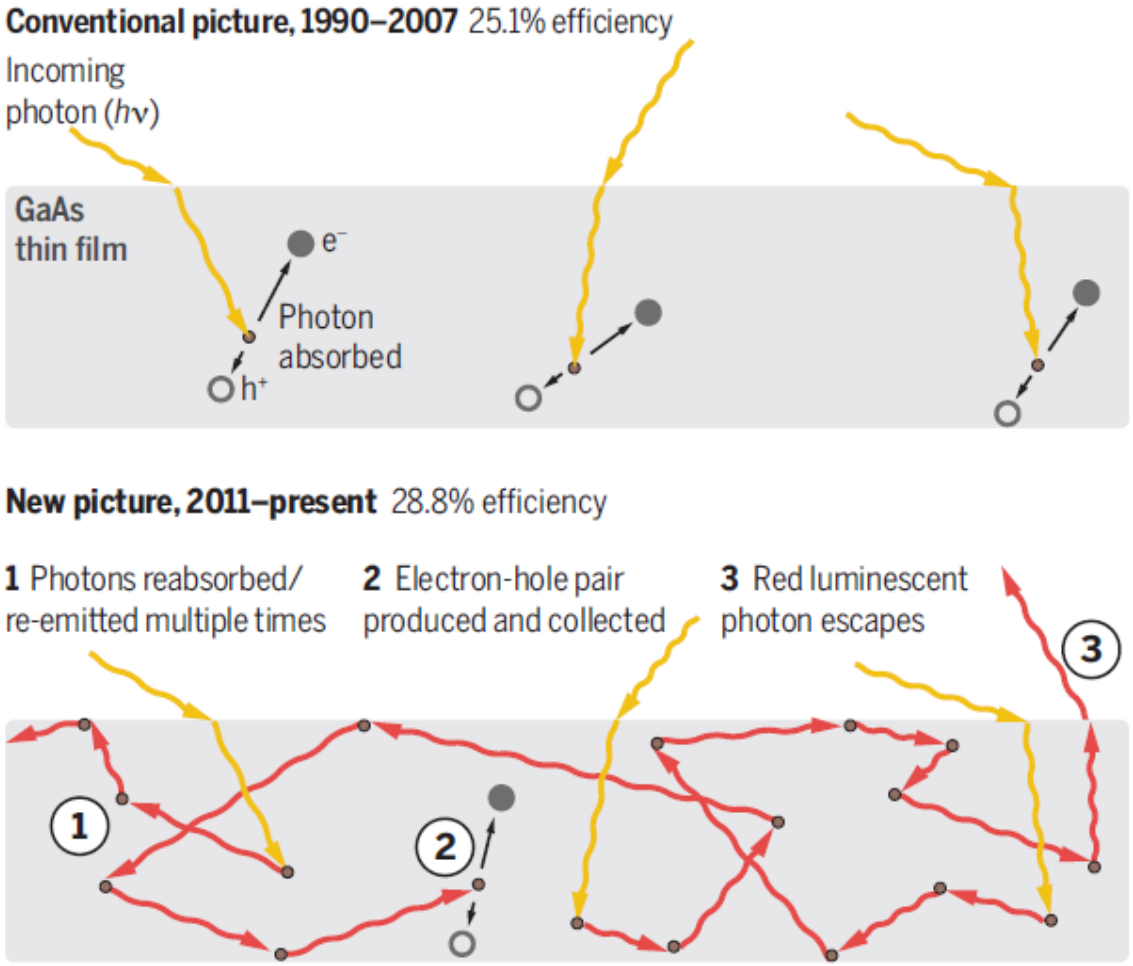

Together with high radiative recombination yields and long carrier lifetimes, these properties raise the question of whether absorption and reemission of excited carriers can occur during the transport. "Photon recycling" does indeed play a central role, allowing considerable increases over current descriptions in the characteristic lengths for charge and energy transport.

Halide Perovskites other than $CH_3NH_3PbI_3$

Pb-free Perovskites

- Replacing Pb with other group IVA elements, Ge, Sn.
- Mixed-(Sn, Pb) perovskites
- Aliovalent ionic pairs replace Pb cations

  $MATl_{0.5}Bi_{0.5}I_3$ (MTBI)

  $MAIn_{0.5}Bi_{0.5}I_3$ (MIBI)

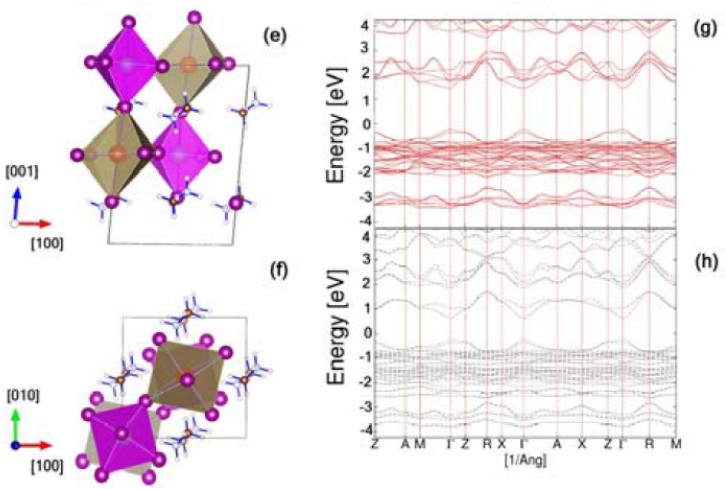

(e)) lateral and (f) top view of the optimized MTBI cell. Bandstructure without (g) and with (h) SOC effect inclusion for MTBI.

Bandgap with SOC
0.84 eV for MTBI.

Reduced effective mass
0.31 (0.33)
Ratio between the two carrier effective masses
0.83 (0.89)
for $MAPbI_3$ (MTBI)

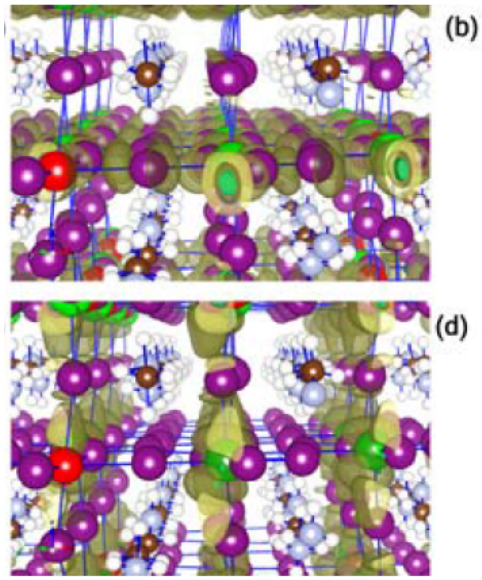

(b) VBM and (d) CBM wavefunctions of MTBI

G. Giorgi, K. Yamashita, Chem. Lett., **44**, 826 (2015).

Computational Screening

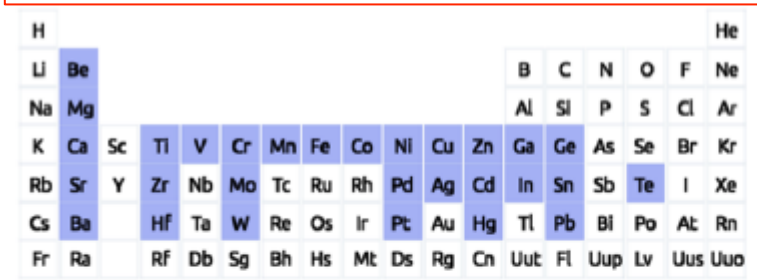

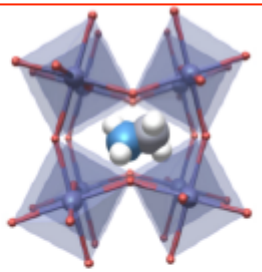

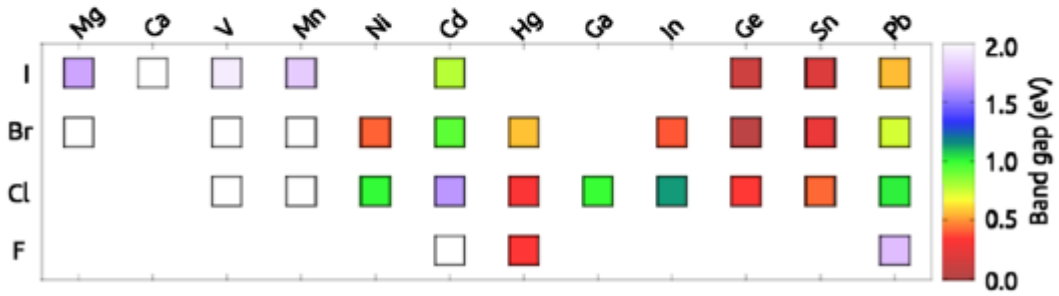

Giustino et al (JPCL 2016)
Woodward et al (CM 2016)
Botti et al (JMCC 2016)

$(MA)_2KBiCl_6$
Indirect band gap 3.02 eV(calc)
3.04 eV(exp)
Cheetham et al
(Mater. Horizons 2016)

Band Gaps of the Lead-Free Halide Double Perovskites $Cs_2BiAgCl_6$ and $Cs_2BiAgBr_6$ from Theory and Experiment

J. Phys. Chem. Lett. 2016, 7, 2579

Marina R. Filip,[†] Samuel Hillman,[‡] Amir Abbas Haghighirad,[‡] Henry J. Snaith,[‡] and Feliciano Giustino*[,†]

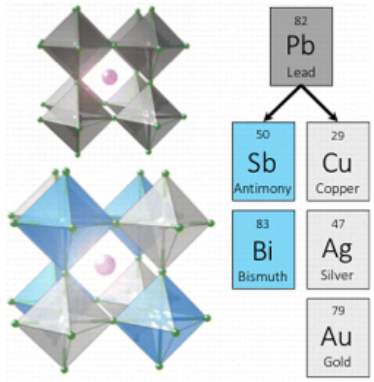

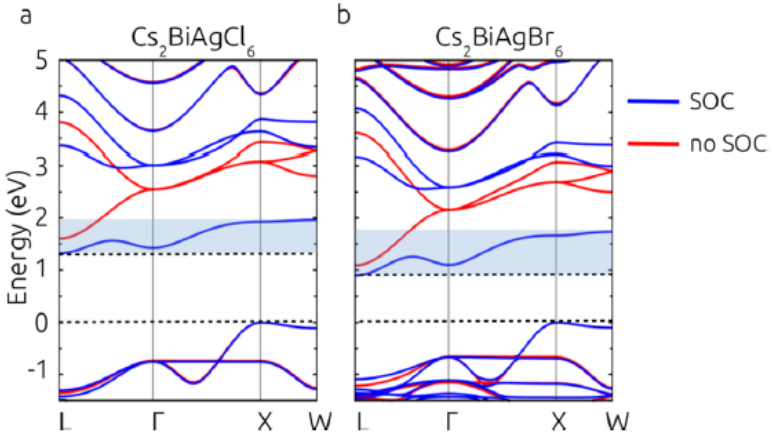

Indirect band gap (eV)

	GW	Exp
$Cs_2BiAgCl_6$	2.2	2.4
$Cs_2BiAgBr_6$	1.8	1.9

Thermal Transport (1)

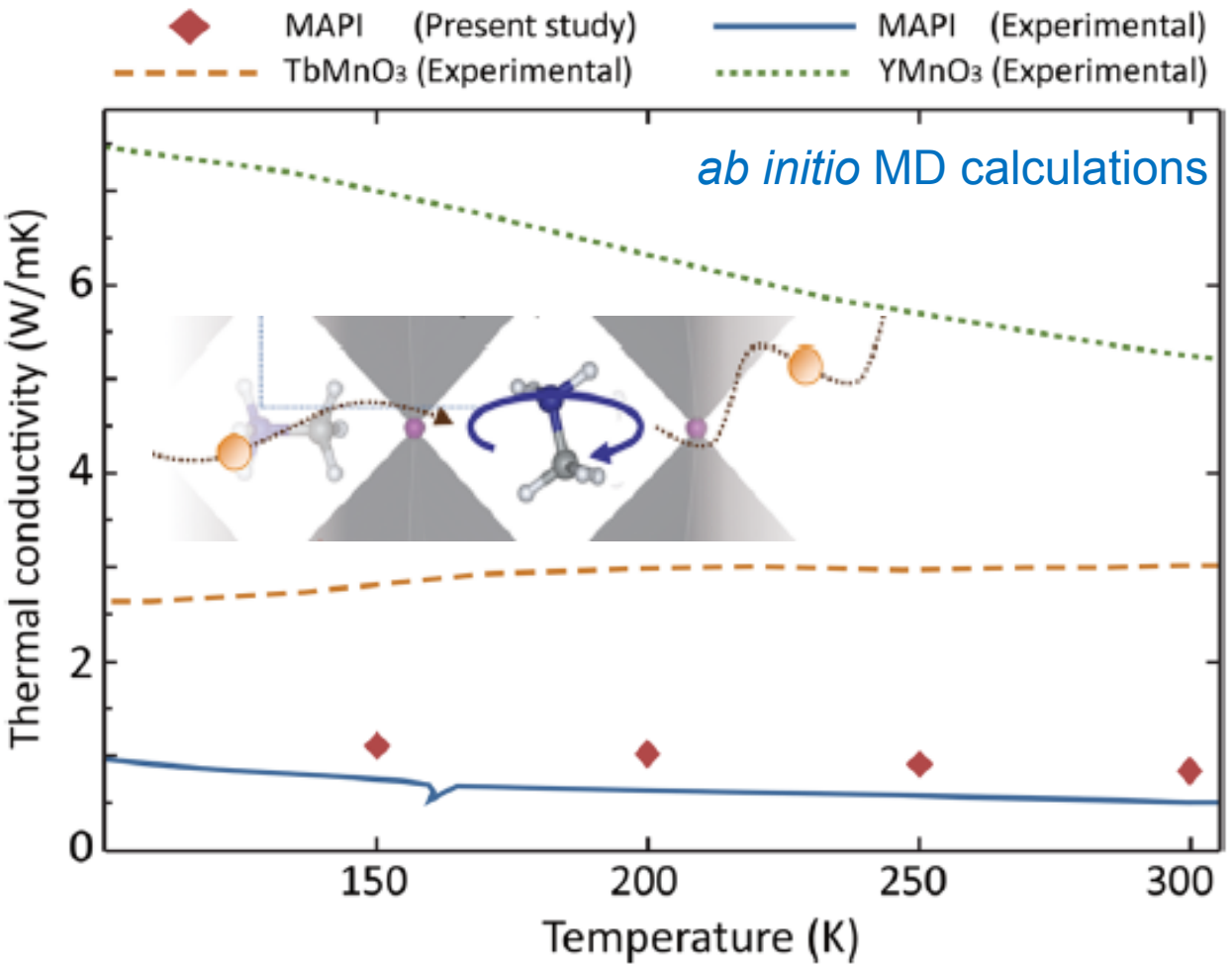

The rotational motion of methylammonium cations is considered responsible for phonon transport suppression.

T. Hata, G.Giorgi, K. Yamashita, *Nano Lett.*, **16**, 2749-2753 (2016)

Thermal Transport (2)

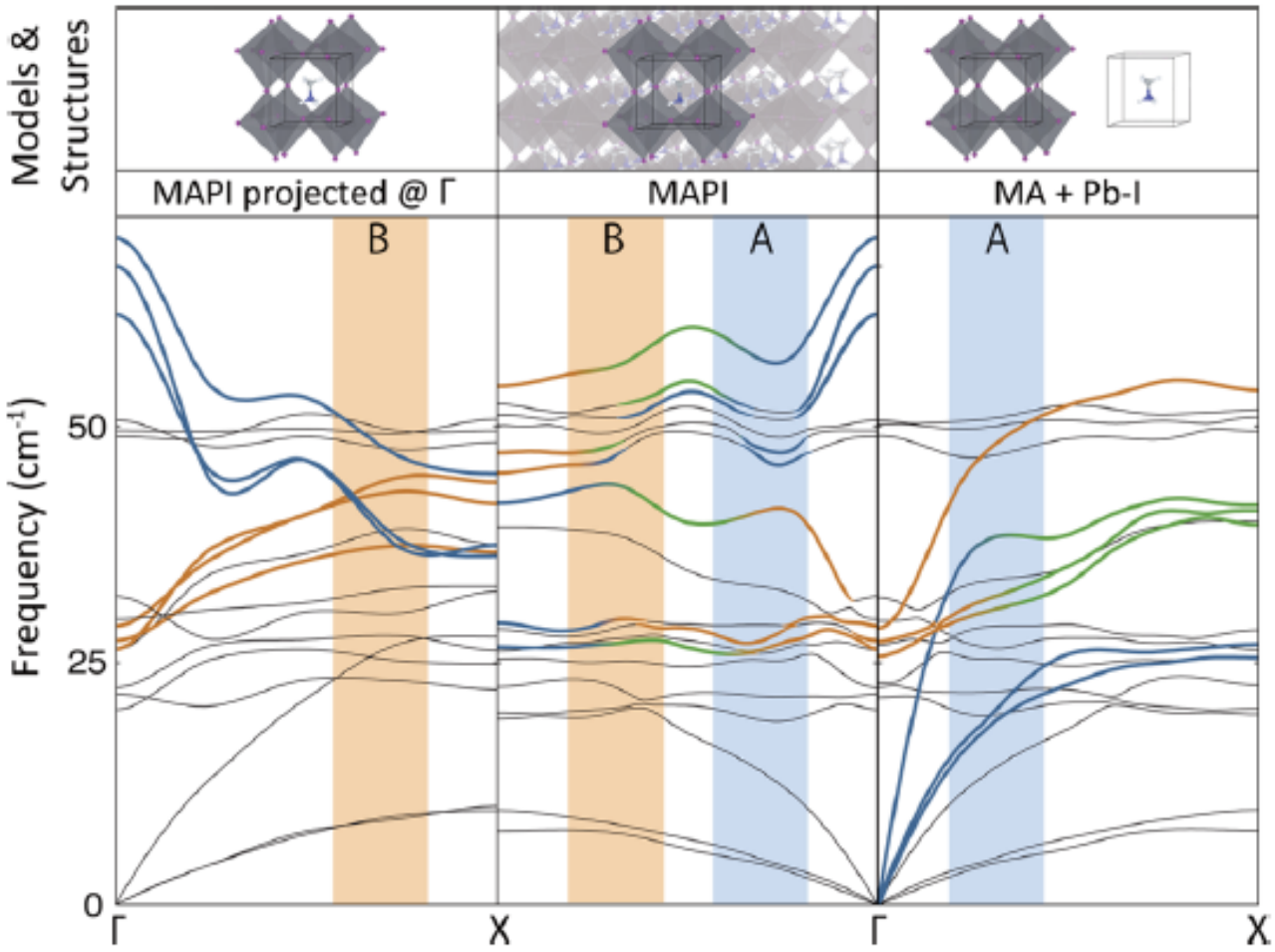

Pb−I
(black thin line)
MA translational
(blue thick line)
rotational
(orange thick line)
mixed motions
(green thick line)

Suppression Mechanism:
the rotations are coupled with translational motions of cations, via which inorganic lattice vibrations are coupled and scatter each other.

T. Hata, G.Giorgi, K. Yamashita, *Nano Lett.*, **16**, 2749-2753 (2016)

Nanostructured OIHPs

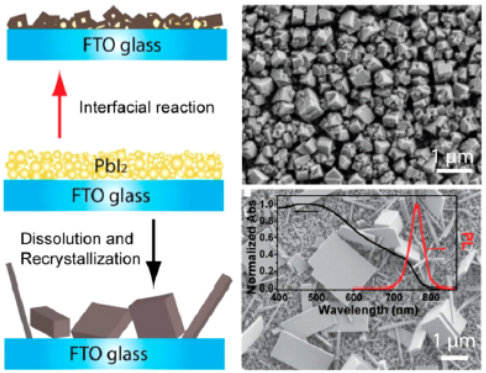

Nanowires, nanorods, nanoplates

Long carrier lifetime

Fu, Jin et al.

J. Am. Chem. Soc. 2015

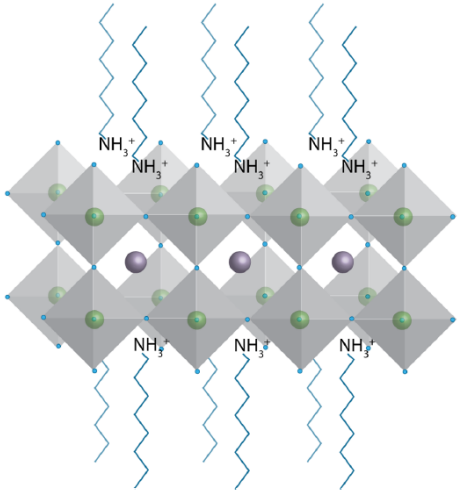

Colloidal Nanoplates

Sharp excitonic absorption

Tyagi, Arveson, Tisdale

J. Phys. Chem. Lett. 2015

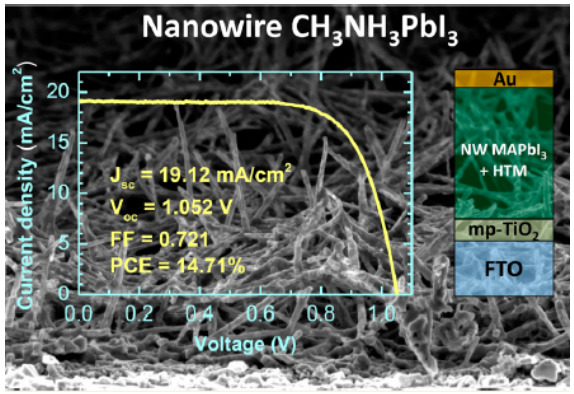

Nanowire

Enhanced excitonic nature

Im, Grätzel, Park et al.

Nano Lett. 2015

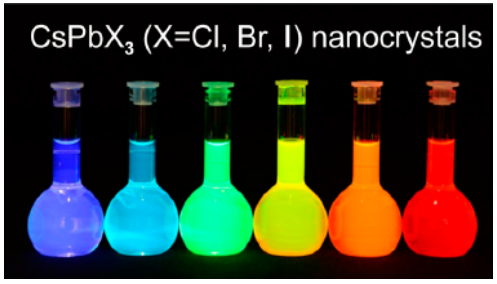

Nanocrystals

Bandgap tunability

Protesescu, Kovalenko et al.

Nano Lett. 2015

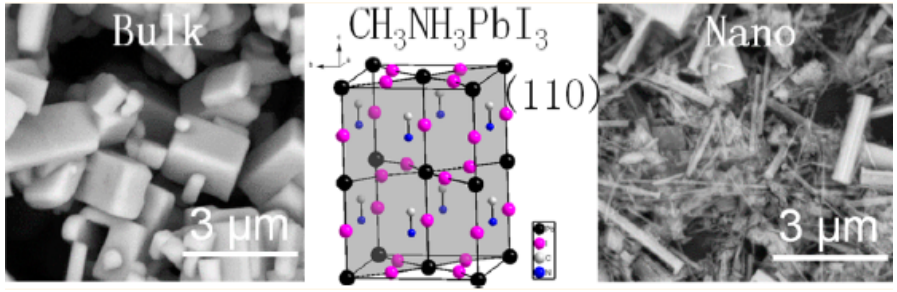

Nanocrystals

Long photoluminescence times

Zhu, Petrich, Smith, Vela et al.

ACS Nano 2015

Averages Volume and Bandgap

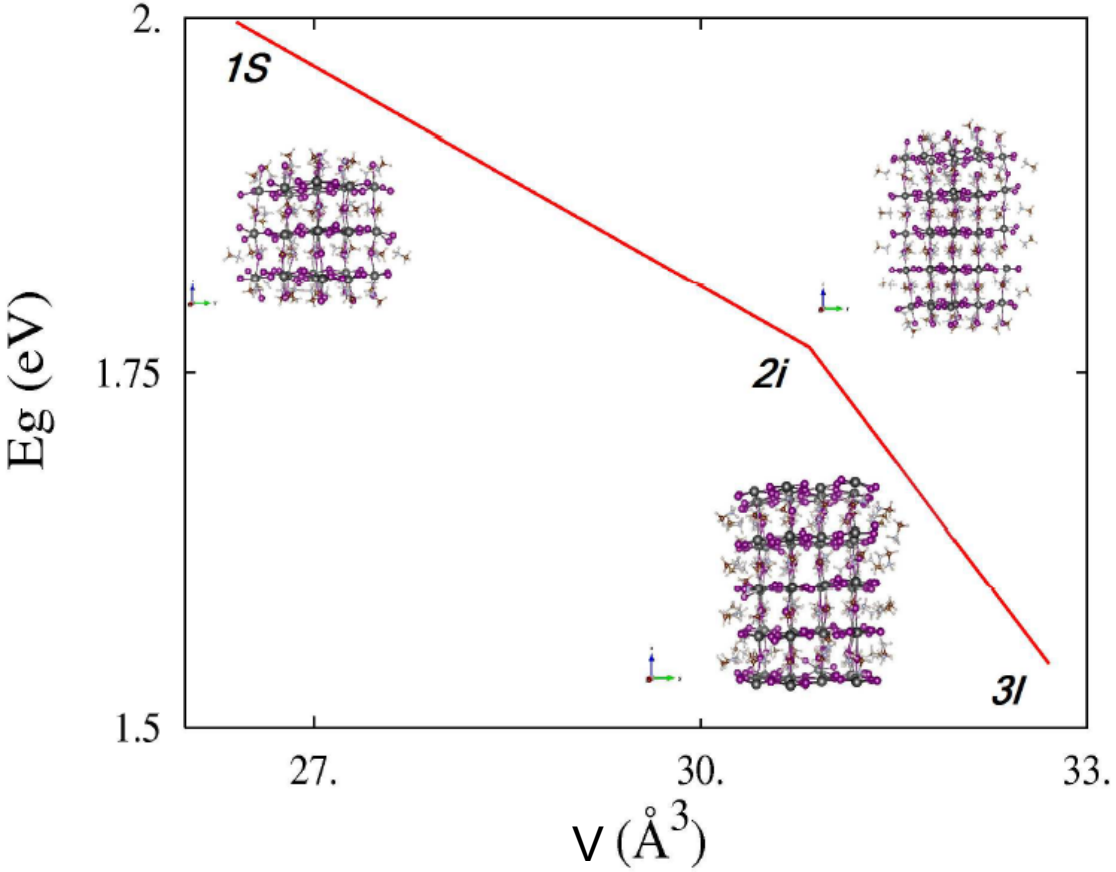

Revealing detectable quantum confinement effects

$$\Delta E_g \approx (2h^2\pi^2/\mu D^2) - (3.6e^2/\varepsilon D)$$

$D = (6V/\pi)^{1/3}$

The calculated average band gap (~1.58 eV) recovers that of the bulk (1.57 eV); an average diameter of 32.7 Å recover the electronic properties of the bulk.

G. Giorgi, K. Yamashita, *J. Phys. Chem. Lett.*, **7**, 888-899 (2016)

Nanoscale Charge Localization Induced by Random Orientations of Organic Molecules in Hybrid Perovskite $CH_3NH_3PbI_3$

Jie Ma and Lin-Wang Wang, *Nano Lett.*, **15**, 248 (2015)

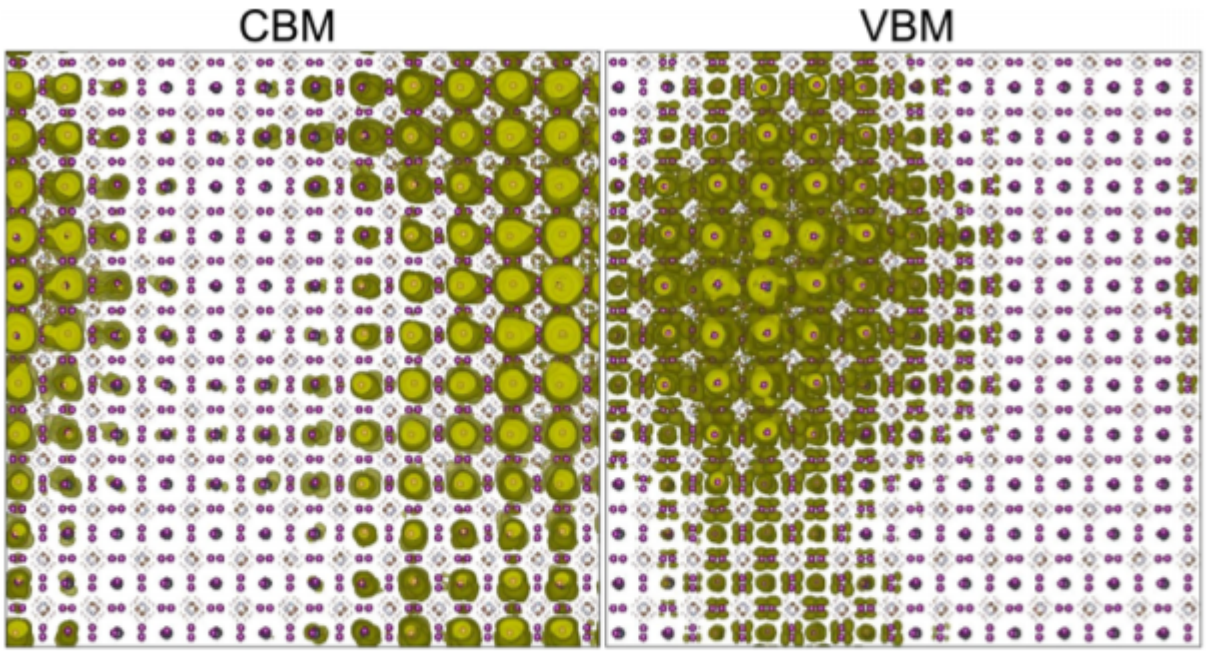

Figure 6. Charge densities of the CBM and VBM states of an equilibrium structure, which is taken from a snapshot of the Monte Carlo simulation at T = 300 K in the 20 736-atom supercell. Both the CBM and VBM are still strongly localized and separated, although the localization sizes increase.